ELSEVIER

Contents lists available at ScienceDirect

Acta Biomaterialia

journal homepage: www.elsevier.com/locate/actbio



Full length article

Mucoadhesive micellar eyedrops for the treatment of ocular inflammation



Yuting Zheng ^{a,1}, Yimin Gu ^{a,1}, Yavuz Oz ^{a,1}, Liangju Kuang ^{b,1}, Ann Yung ^b, Seokjoo Lee ^b, Reza Dana ^b, Nasim Annabi ^{a,c,*}

- a Department of Chemical and Biomolecular Engineering, University of California, Los Angeles, Los Angeles, CA, 90095, United States
- b Schepens Eye Research Institute of Massachusetts Eye and Ear, Department of Ophthalmology, Harvard Medical School, Boston, MA, USA
- ^c Department of Bioengineering, University of California, Los Angeles, Los Angeles, CA, 90095, United States

ARTICLE INFO

Keywords: Micellar drug delivery Mucoadhesion Eyedrops Anti-inflammatory Ocular inflammation

ABSTRACT

Efficient ocular drug delivery remains a significant challenge in treating eye inflammation due to physiological barriers such as the tear film and frequent blinking, which lead to rapid drug clearance. Commercial eyedrops, like Oceanside® (0.5 % loteprednol etabonate (LE) ophthalmic suspension), suffer from low ocular bioavailability and require frequent dosing to maintain therapeutic levels. To address these limitations, we developed a mucoadhesive micellar drug delivery system to enhance the bioavailability and retention of LE on the cornea. Our system employed polymeric micelles (MCs) functionalized with phenylboronic acid (PBA), which exhibited high conjugation efficiency to enable strong binding to the mucin-rich corneal layer. These MCs were synthesized using PBA-functionalized poly (ethylene glycol)-b-poly (N-(2-hydroxypropyl) methacrylamide-oligolactate) (PBA-PEG-b-p(HPMA-Lacm)) and subsequently dispersed into a shear-thinning matrix solution to form a micellar eyedrop formulation. The resulting eyedrop demonstrated a sustained LE release over 12 days, enabling prolonged therapeutic exposure. In vitro, ex vivo, and in vivo studies confirmed enhanced mucoadhesion and extended corneal retention. The formulation was biocompatible with human corneal epithelial cells and demonstrated ocular safety in mice. In a murine model of electrocautery-induced corneal inflammation, a oncedaily administration of LE-loaded PBA-MC eyedrops significantly reduced corneal opacity, preserved corneal structure, and lowered immune cell infiltration and cytokine levels. Notably, the therapeutic efficacy of the LEloaded PBA-MC eyedrops matched that of commercial Oceanside®, which required four daily doses. These findings suggest that the engineered PBA-MC eyedrops could serve as a promising platform for ocular drug delivery, addressing the challenges associated with treating eye inflammation effectively.

Statement of significance: Mucoadhesive nanoparticles used for ocular drug delivery often suffer from low attachment efficiency, limiting their effectiveness. Additionally, the lack of *in vivo* comparisons with commercial eye drops hinders evaluating their clinical benefits.

To address these issues, we developed PBA-functionalized polymeric MCs to enhance the bioavailability of LE by increasing its retention on the corneal mucin layer. These MCs showed high PBA conjugation efficiency, a 12-day sustained release of LE, strong mucin adhesion, *in vitro* and *in vivo* biocompatibility. In a mouse model of corneal inflammation, a once-daily LE-loaded micellar eyedrop matched the efficacy of the commercial LE eyedrop (Oceanside®, 0.5 %), which was dosed four times daily, reducing corneal opacity, preserving corneal structure, and decreasing inflammation.

1. Introduction

Eye inflammation, a prevalent condition characterized by redness, swelling, and patient discomfort, can lead to serious consequences, including vision loss or blindness, especially if left untreated [1,2].

Inflammation in the eye, if not properly managed, can cause damage to various structures within the eye, such as the cornea, retina, and optic nerve, which are essential for vision. For example, untreated inflammation can lead to conditions like uveitis, which can result in vision impairment or even permanent vision loss if not promptly treated [2].

Received 11 June 2024; Received in revised form 19 May 2025; Accepted 27 May 2025 Available online 28 May 2025

1742-7061/© 2025 The Authors. Published by Elsevier Inc. on behalf of Acta Materialia Inc. This is an open access article under the CC BY license (http://creativecommons.org/licenses/by/4.0/).

^{*} Corresponding author at: Department of Chemical and Biomolecular Engineering, University of California, Los Angeles, Los Angeles, CA, 90095, United States. E-mail address: nannabi@ucla.edu (N. Annabi).

 $^{^{1}}$ These authors contributed equally.

Additionally, chronic inflammation in the eye may contribute to the development or progression of other eye conditions, such as glaucoma or cataracts, further highlighting the importance of early detection and appropriate treatment [3–5]. The current standard of care for treating eye inflammation involves traditional methods such as ointments and eyedrops [6,7]. However, these treatments encounter challenges in effectively delivering therapeutic doses to the cornea, which can be due to ocular barriers and low drug retention in the cornea. Consequently, frequent application of eyedrops becomes necessary, leading to reduced patient compliance. Moreover, the bioavailability of anti-inflammatory drugs is limited due to their hydrophobic nature, with <5 % reaching the intended target site [8,9].

To overcome these challenges, various ocular drug delivery systems have been developed as alternatives to current treatment methods, including adhesive hydrogels [10-12], nanoparticles (NPs) [13-17], microneedles [18-21], and drug-eluting contact lenses [22-25]. These systems primarily aim to prolong drug retention on the ocular surface. Although these methods present opportunities for more efficient treatment of ocular inflammation by improving drug bioavailability, they still face several obstacles. For example, advanced delivery systems, such as drug-eluting adhesive hydrogels, microneedles, and contact lenses, offer innovative solutions for ocular drug delivery, but they often struggle with effective delivery of hydrophobic drugs, fast drug release, and complexity [26,27]. Traditional methods such as eyedrops are easy to use but may fall short in providing a sustained drug release profile, requiring multiple applications per day. Bridging this gap with a platform that combines the convenience of eyedrops with a sustained drug release profile would be immensely valuable in clinical practice for improving patient outcomes and treatment efficacy.

In recent years, NPs have gained attention as a preferred drug delivery system due to their high drug encapsulation efficiency and precise control over drug release [28]. Among various nano-delivery systems, polymeric micelles (MCs), formed through the self-assembly of amphiphilic polymers in an aqueous environment, allow to efficiently encapsulate hydrophobic drug molecules within their cores to improve their solubility [29]. However, the use of drug loaded MCs for treatment of eye inflammation encounter challenges such as rapid clearance from the ocular surface caused by frequent blinking and tear flow, requiring robust MC mucoadhesion for sustained drug delivery [17,30]. Surface modification of polymeric MCs with suitable mucoadhesive groups can address this limitation by providing a robust adhesion to the ocular surface.

Among various mucoadhesive moieties, phenylboronic acid (PBA) stands out as it offers satisfactory chemical stability for mucin targeting [31]. The efficacy of PBA-functionalized nano-drug carriers in treating various eye diseases such as dry eye syndrome and fungal keratitis, has been previously demonstrated, showing promising in vitro and in vivo ocular targeting outcomes attributed to PBA grafting [32-34]. Despite these promising findings, several challenges hinder the clinical translation of PBA-functionalized NPs. One significant challenge is the low efficiency of PBA conjugation, which can impact the overall effectiveness of the nano-drug carriers [16,32]. For instance, Gu et al. developed PBA-functionalized poly(D,L-lactide)-b-dextran (PLA-b-Dex) self-assembles into NPs. However, the PBA conjugation efficiency was reported to be only 17.6 %. Moreover, the PBA density must be carefully optimized to strike a balance between mucoadhesion and colloidal stability [16]. Additionally, lack of in vivo data comparing the efficacy of these PBA-functionalized NPs with commercial eye drops makes it challenging to evaluate the potential advantages of these PBA-functionalized carriers for clinical translation. In another study, the Sheardown group synthesized and characterized a series of poly(L-lactide)-b-poly(methacrylic acid-co-3-acrylamidophenylboronic acid) block copolymer MCs as mucoadhesive drug delivery vehicles. Although this platform exhibited 65 % PBA conjugation efficiency and a sustained drug release profile, reduced cell proliferation and altered cell morphology were observed in the MC-treated group. Moreover, the

therapeutic efficacy of this platform was not demonstrated [8]. Lastly, achieving a sustained release profile remains a challenge. The state-of-the-art mucoadhesive micellar/liposomal ocular drug delivery systems developed thus far with their limitations including low PBA conjugation efficacy, fast drug release profile, and low *in vitro* biocompatibility are summarized in **Table S1**. There is an urgent need to develop a mucoadhesive drug delivery system with high PBA conjugation for sustained delivery of hydrophobic drugs.

Among medications for ocular inflammation, loteprednol etabonate (LE) may induce less intraocular pressure compared to other steroids like dexamethasone (DEX) and prednisolone acetate [35–37]. Moreover, LE enables rapid metabolism post-activation, reducing the risk of adverse effects due to its ester at carbon 20, in contrast to a ketone group found in other ophthalmic corticosteroids [38,39]. However, efficient loading of LE into NPs presents challenges, likely due to its highly lipophilic nature, which surpasses that of DEX by ten-fold [39,40]. Hence, the development of an effective strategy for loading and sustained delivery of LE is essential to ensure better bioavailability in the ocular tissue.

To address the demand for effective delivery of anti-inflammatory drugs and overcome the challenge of NP retention on ocular surfaces, we introduced an innovative mucoadhesive micellar eyedrop for sustained delivery of LE. We utilized an amphiphilic block copolymer with a PBA end group, named PBA-functionalized poly (ethylene glycol)-b-poly (N-(2-hydroxypropyl) methacrylamide-oligolactate) (PBA-PEG-b-p (HPMA-Lac_m)), to engineer mucoadhesive MCs with high PBA conjugation efficiency. Mucoadhesion property and drug release profile of PBA-MC eyedrops were evaluated. Additionally, we assessed the biocompatibility of PBA-MC eyedrops in vitro using human corneal epithelial cells and in vivo using a healthy mouse model. Finally, we employed a mouse model of electrocautery-induced corneal inflammation to demonstrate effectiveness of LE loaded PBA-MC (PBA-MC-LE) eyedrops in vivo, thoroughly evaluating the clinical potential of this platform.

2. Experimental section

Materials: Tert-butyloxycarbonyl (tBoc) protected amine polyethylene glycol (tBoc-NH-PEG-OH, MW 3.4k) was purchased from Biopharma PEG Scientific Inc. PBA, LE, (3S)-cis-3,6-dimethyl-1,4-dioxane-2,5-dione (L-lactide), 4,4'-Azobis(4-cyanovaleric acid) (ACVA), 4-(Dimethylamino)pyridine (DMAP), p-toluenesulfonic acid (pTS), Sn (Oct)2, bovine serum albumin (BSA), and porcine gastric mucin were purchased from Sigma-Aldrich. Hydroxypropyl methacrylate (HPMA) was purchased from Polysciences, Inc. 4-methoxyphenol was purchased from Acros Organics Chemicals. N,N'-Dicyclohexylcarbodiimide (DCC), 1-ethyl-3-(3-dimethylaminopropyl) carbodiimide (EDC) and N-hydroxysuccinimide (NHS) were purchased from Tokyo Chemical Industry Co., Ltd. (TCI Chemicals). Acetonitrile (ACN), ethyl acetate, hexane, cyclohexane, tetrahydrofuran (THF), ethanol, methanol, dimethyl sulfoxide (DMSO), methylene chloride (DCM), trifluoroacetic acid (TFA), chloroform-d (CDCl₃), and deuterated dimethyl sulfoxide (CD₃)₂SO) were purchased from Fischer Scientific. Human corneal epithelial cells (PCS-700-010) were generated by Dr. Argueso's lab. Alveolar epithelial cell medium was purchased from ScienCell. Live/Dead™ Viability/ Cytotoxicity Kit, Alexa Fluor 594-phalloidin, and DAPI were purchased from Invitrogen.

Synthesis and Characterization of PBA-PEG-OH: A solution of HO-PEG-NH $_2$ (105 mg) was prepared in 0.8 mL of 0.1 M MES buffer at pH 6. Separately, EDC (148 mg) was dissolved in 0.1 mL MES buffer and added to PBA (25.5 mg) dissolved in 0.1 mL of DMSO. This mixture was stirred at 45 °C for 20 min, followed by the dropwise addition of NHS (35.5 mg) dissolved in 0.1 mL of MES buffer. The mixture was then stirred at 45 °C for 1–2 h to activate the carboxyl functional group on PBA. Subsequently, the HO-PEG-NH $_2$ solution was added dropwise to this mixture, and the pH was adjusted to 7 using NaOH. The reaction was allowed to

proceed for 14 h at 25 °C. The product was purified by dialyzing Milli-Q water for 5 days and obtained by freeze-drying.

Synthesis of PBA-PEG-ACVA Macroinitiator: The macroinitiator was synthesized through an esterification reaction between PBA-PEG-OH (500 mg) and ACVA (20.6 mg) in 5 mL of anhydrous DCM. DMAP (5.4 mg) and pTS (8.4 mg), dissolved separately in 0.1 mL of anhydrous THF, were added into the reaction mixture and stirred in an ice bath for 30 min, while purging with nitrogen. Then, DCC (84.6 mg), dissolved in 0.5 mL of anhydrous DCM, was added dropwise to the reaction mixture at 0 °C. The mixture was allowed to warm to 25 °C and stirred for 16 h. The urea salts were removed through filtration, and the remaining mixture was vacuum-dried. Finally, the solid product was dissolved in Mili-Q water and further purified by dialysis against Mili-Q water.

Synthesis and Characterization of HPMA-Lac_m Monomer: HPMA-Lac_m monomer was synthesized following a previously reported method [41]. In summary, L-lactide (5.0 g), HPMA (2.5 g), Sn (Oct)₂ (35.1 mg) and sodium sulfate (5 mg) were added to a round bottom flask. The flask was subjected to vacuum/N₂ gas cycle at least three times to remove air. Subsequently, the flask was heated to 110 °C while stirring until complete dissolution of solids was achieved. The mixture was allowed to react at 110 °C for 18 h. After the reaction, the mixture was cooled to 25 °C and dissolved in THF. This solution was then precipitated into cyclohexane to remove any unreacted reagents. Finally, the precipitate dried under vacuum overnight.

Synthesis of PBA-PEG-b-p(HPMA-Lac_m) Copolymer: The diblock copolymer PBA-PEG-b-p(HPMA-Lac_m) was synthesized through a free radical polymerization [42], with a slight modification. Synthesis of the monomer can be found in supporting information. During the polymerization process, a molar ratio of monomer:macroinitiator = 200:1 was applied. They were dissolved in anhydrous ACN, and purged with nitrogen for 20 min. The mixture was then immersed in an oil bath at 70 °C for 24 h. To terminate the polymerization, the mixture was exposed to the air after 24 h. Subsequently, the copolymer was precipitated into cold diethyl ether and collected by centrifugation. This purification step was repeated at least three times to obtain a pure PEG-b-p(HPMA-Lac_m) copolymer.

Fabrication of Drug-loaded and Unloaded MCs: Drug-loaded MCs were prepared by a solvent evaporation method. Initially, 10 mg of copolymer with and without PBA end group (dissolved in 970 μL of acetone) and 1 mg of LE (dissolved in 30 μL DMSO) were mixed and incubated at 37 °C for 30 min. The copolymer-drug mixture was then added dropwise into the AAB (120 mM, pH = 5), followed by stirring at 25 °C for 30 min. Subsequently, the mixture was stirred at 45 °C for 2 h. To facilitate the evaporation of acetone, the vial was uncapped and stirred overnight at 25 °C. Unloaded MCs, both PBA-MC and NH2–MC, were prepared using the same method but without adding the drug.

Critical Micelle Concentration (CMC) Determination: CMC of the engineered MCs was determined using an established pyrene fluorescence probe method [43,44]. Briefly, the block PBA-PEG-b-p(HPMA--Lac_m) copolymer was dissolved in 500 µL THF and added slowly to 4.5 mL of 120 mM ammonium acetate buffer (AAB) (final polymer concentration ranging from 1 to 1×10^{-6} mg/mL). The dispersions were stirred for 2 h at room temperature to evaporate THF. Next, 15 μL of pyrene dissolved in acetone (concentration: $1.8 \times 10^{-4} \, \text{M}$), was added, and the mixtures were incubated at room temperature for 20 h to allow the evaporation of acetone. Fluorescence excitation spectra of pyrene were obtained by a Tecan Infinite M200 Pro Microplate Reader at an angle of 90° The excitation spectra were recorded at 37 °C (from 300 to 360 nm with an emission wavelength of 390 nm). The excitation and emission band slits were 4 and 2 nm, respectively. The intensity ratio of I_{338}/I_{333} was plotted against the polymer concentration to determine the CMC.

In Vitro Biocompatibility Test: The cytocompatibility of the engineered PBA-MC and matrix was assessed by examining the *in vitro* viability and metabolic activity of human corneal epithelial cells. To evaluate cell viability and proliferation, a commercial Live/Dead kits

(Invitrogen) and Actin/(4',6-diamidino-2-phenylindole) DAPI staining (Invitrogen) were employed. Additionally, a PrestoBlue assay (Life Sciences) was conducted to evaluate the metabolic activity of the cells. Human corneal epithelial cells were seeded at a density of 1×10^4 cells/ cm² on the bottom of a 48-well plate. Each well, containing PBA-MC in the matrix at a concentration of 3 % (w/v), received 300 µL of growth medium (Dulbecco's Modified Eagle's Medium). The well plates were maintained at 37 °C in a humid 5 % environment for 5 days, with the culture medium and PBA-MC eyedrops replaced every 48 h. Cell viability was examined using a Live/Dead viability kit according to the manufacturer's instructions (n = 4). Briefly, cells were stained with 0.5 $\mu L/mL$ of calcein AM and 2 $\mu L/mL$ of ethidium homodimer-1 (EthD-1) in DPBS for 20 min at 37 °C. Fluorescent imaging was performed on the first and fifth day post-seeding using an AxioObserver Z7 inverted microscope. Live and dead cells were visualized by their green and red colors, respectively, and quantified using CellProfiler $^{\text{TM}}$ software. Cell viability was determined as the number of live cells divided by the total number of cells.

The metabolic activity of the cells was assessed on days 1, 3, and 5 using a PrestoBlue assay (Life Technologies) (n=6). Human corneal epithelial cells were incubated in 200 μ L of 10 % (v/v) PrestoBlue reagent in growth medium for 45 min at 37 °C. Fluorescence was measured using a Synergy HT fluorescence plate reader (BioTek).

To observe the spreading of human corneal epithelial cells at the bottom of the 48-well plates (n=4), F-actin/cell nuclei staining was performed. Cells at days 1 and 5 post-seeding were fixed in 4 % (v/v) paraformaldehyde (Sigma) for 15 min, permeabilized in 0.1 % w/v Triton X-100 (Sigma) for 5 min, and blocked in 1 % (w/v) bovine serum albumin (BSA, Sigma) for 30 min. Subsequently, the samples were incubated with Alexa Fluor 488 phalloidin for 45 min. After repeated washes with DPBS, the samples were counterstained with 1 μ L/mL of DAPI in DPBS for 2 min, and fluorescent imaging was conducted using an inverted fluorescence microscope (Zeiss Axio Observer Z7).

In Vitro Anti-inflammatory Study: The in vitro anti-inflammatory assessment was performed using a previously published protocol [45]. RAW 264.7 cells were seeded in 48-well plates at a density of 2 \times 10⁴ cells/well and cultured for 24 h in a culture medium. Macrophage activation was induced by adding 4 µg/mL lipopolysaccharide (LPS) (Invitrogen, Thermo Fisher Scientific) to the media for 24 h. Following induction, different treatment groups (2 µL each) were added to the media for 48 h to assess their anti-inflammatory effects: 1) Cell only (no treatment); 2) Cell + LPS; 3) Cell + LPS + PBA-MC; 4) Cell + LPS + PBA-MC-LE; 5) Cell + LPS + Matrix; and 6) Cell + LPS + PBA-MC-LE + Matrix (n = 5 per group). To evaluate the anti-inflammatory effects, the expression of the M1 phenotypic marker CD80 was detected using fluorescence microscopy. After treatment, the cells were fixed with 4 % paraformaldehyde for 10 min, followed by washing with DPBS. The cells were then blocked with 5 % goat serum solution for 1 h at room temperature. After blocking, the cells were incubated with an anti-CD80 antibody (Invitrogen, Thermo Fisher Scientific), and diluted in 5 % goat serum for 2 h. Following further DPBS washing, the cells were stained with DAPI solution to visualize the nuclei. Finally, the cells were observed and photographed using a fluorescent microscope (Zeiss Axio Observer Z7).

Eyedrop Formulation and Characterization: The composition of the matrix eyedrops included active ingredients such as hyaluronic acid (HA) (0.5 %), glycerin (0.3 %), hypromellose (0.3 %), and inactive ingredients: boric acid (0.8 %), calcium chloride (0.0053 %), magnesium chloride (0.0065 %), benzalkonium chloride (0.0065 %), potassium chloride (0.038 %), sodium chloride (0.4 %), and zinc chloride (0.00015 %). The pH of the final mixture was adjusted to 7.4. The rheological properties of the matrix were examined using a Modular Compact Rheometer MCR302. Results were obtained by connecting the measuring system PP08 with an 8 mm diameter to the rheometer. Each measurement involved loading a fresh sample into the 1 mm gap between the parallel plates and removing excess samples. The viscosity

and shear stress relationship as a function of shear rate was recorded at various shear rate parameters, ranging from 1 to 1000 s $^{-1}$, with 30 measuring points.

Proton Nuclear Magnetic Resonance (1H NMR)Spectroscopic Analysis: The 1H NMR analysis on PBA-PEG-OH, PEG-ACVA, PBA-PEG-ACVA, HPMA-Lac_m monomer, PBA-PEG-b-p(HPMA-Lac_m), NH₂-PEG-b-p (HPMA-Lac_m) was conducted using a Brucker AV 400 MHz NMR Spectrometer (32 scans, 2-second delay). The chemical shifts of CDCl₃ at 7.26 ppm and (CD₃)₂SO at 2.50 ppm were used to calibrate the reference line. The percent conjugation efficiency of PBA onto NH₂-PEG, the number of average Lac repeating units (m), the number of hydrophobic blocks (x), and the average molecular weight of copolymer (Mw_{cop}) were determined by 1H NMR using the following Eqs. (1–4):

Conjugation Efficiency (%) =
$$\frac{I_{benzen-H} / 4}{I_{PEG-H} / 296} \times 100$$
 (1)

$$m = \frac{I_{\text{Lac repeat unis-H}}}{I_{\text{Lac repit II}}}$$
 (2)

$$x = \frac{I_{Lac\ tail-H} / 1}{I_{PEG-H} / 296}$$
 (3)

$$Mw_{cop} = Mw_{PEG} + [(x) \times Mw_{HPMA-Lac}]$$
 (4)

 $I_{benzen-H}$ represents the integration of the total areas of the 4 benzene protons on the PBA. I_{PEG-H} corresponds to the integrated area of 296 protons on PEG repeating units. $I_{Lac\ repeat\ units-H}$ denotes the integrated area of Lac repeating units —[COCH(CH₃)O]— (at 5.12 – 5.26 ppm), and $I_{Lac\ tail-H}$ represents the integrated area of the proton at the tail —COCH(CH₃)OH (at 4.30 ppm) of the HPMA-Lac_m monomer.

Dynamic Light Scattering (DLS)and Zeta Potential Characterizations of MCs: Freshly prepared micellar dispersions were concentrated using a protein concentrator, diluted with DPBS (pH = 7.4), and filtered with a 0.45 μm filter. The sizes of the MCs were analyzed using DLS on a Malvern Zetasizer Nano-Z instrument (Malvern Instruments, Malvern, UK). Three measurements were performed for each sample under standard operating procedure parameters (25 $^{\circ}C$ with 20-second equilibration time).

The Zeta potential of the MCs was determined at 25 $^{\circ}$ C using a Malvern Zetasizer Nano-Z (Malvern Instruments, Malvern, UK) equipped with universal ZEN 1002 'dip' cells and DTS (Nano) software (version 4.20). Zeta potential measurements were performed in DPBS at pH 7.4 at a final MC concentration of 333 μ g/mL.

Transmission Electron Microscope (TEM)Characterization of MCs: The TEM images of MCs were taken using T12 Quick room temperature TEM with a 120 kV electron-beam energy. The samples were dispersed in Milli-Q water, then dropped and dried on carbon-coated copper grids.

Assessment of Drug Encapsulation Efficiency (EE %) and Loading Capacity (LC %) of MCs: The amount of the loaded LE within the polymeric MCs was determined using high-performance liquid chromatography (HPLC). A standard curve was obtained using LE dissolved in ACN at concentrations ranging from 0.01 to 0.1 mg/mL. The concentration of LE solutions was measured using HPLC with an ACN/water without acid gradient solvent system at 242 nm. Column (5C18-MS-II, 4.6ID x 250 mm) was used at 1 mL/min flow rate, with a 70 %–90 % acetonitrile gradient for 10 min. The set inject volume into the HPLC was 5 μ L per sample. The freshly prepared drug loaded MCs were centrifuged at 4000 rpm at 20 °C for 10 min to separate unencapsulated LE pellet. Following the centrifugation process, the supernatant was carefully pipetted out. The LE pellet was dissolved in 10 mL of acetonitrile. The EE % and LC % were calculated using Eqs. (5) and (6), respectively:

$$EE\% = \left(1 - \frac{\text{unencapsulated drug}}{\text{total drug added}}\right) \times 100\%$$
 (5)

$$LC\% = \left(1 - \frac{unencapsulated \ drug}{total \ copolymer \ added}\right) \times 100\% \tag{6}$$

Drug Release Studies: After removing unencapsulated LE pellet through centrifugation, the supernatant was concentrated to 100 µL using a protein concentrator with a specified molecular weight cutoff (MWCO 20 kDa). Subsequently, drug loaded MC solution was mixed with 900 uL of an evedrop solution. For the release study, 1 mL of MCs dispersed in evedrop solution was pipetted into a dialysis bag (MWCO 12 kDa), and the bag was submerged in 10 mL of artificial tear solution placed in a falcon tube. The falcon tube was then placed in a shaker at 37 °C and gently shaken at 80 rpm for 12 days. To monitor the release of LE into the artificial tear solution, 2 % (v/v) non-ionic surfactant Triton X-100 was added to the solution to enhance the solubility of LE. At predetermined time intervals (0 h, 2 h, 6 h, 24 h, 2 days, 3 days, 5 days, 7 days, 9 days, and 12 days), 2 mL artificial tear was sampled, and an equal volume of fresh release media was replenished. The release samples were freeze-dried, re-dissolved in ACN, and their concentration was measured by HPLC using the same method described previously. The composition of artificial tear fluid used was sodium chloride 0.670 g, sodium bicarbonate 0.200 g, calcium chloride 2H2O 0.008 g, purified water q.s. 100.0 g [46].

Mucoadhesion Experiments via Turbidity: Porcine gastric mucin was prepared as a 1 mg/mL solution with Mili-Q water using a probetype sonicator (FisherBrand) at 500 W, 20 kHz. Sonication was performed at a 5-second interval until the mucin was completely dissolved. PBA-MC and NH_2 -MC were suspended in DPBS (1 mg/mL, pH = 7.4). The MC and mucin solutions were mixed to achieve various MCs to mucin ratios (0.1, 1, 2, 3, 10) and vigorously vortexed for 1 min. The optical density at 600 nm (OD₆₀₀) of DPBS and MCs/mucin solutions were measured by a UV-vis spectrophotometer (Thermo Scientific, NanoDrop One).

Mucoadhesion Experiments via Fluorescent Spectrometer: PBA-MC were mixed with varying concentrations (0, 0.02, 0.05, 0.1, 0.2, 0.5 mM) of sialic acid solutions to achieve constant final concentration of PBA-MC (50 μ g/mL). The mixtures were vortexed for 30 s before measurement with a plate-reader-type fluorescent spectrometer (Tecan Infinite M1000 Pro). The samples were excited at 295 nm, and an emission scan from 335 to 435 nm was obtained for each sample.

Ex Vivo Mucoadhesion Characterization: For the ex vivo drug retention study, the eyeballs of the rabbits were taken out and immediately treated with LE loaded PBA-functionalized MCs (0.25 % (w/v) LE) and commercial LE eyedrops (EYSUVIS®, 0.25 % (w/v)), followed by incubation for 15 min based on a previously developed protocol [47, 48]. The eyeballs were washed vertically with artificial tears at a rate of 1 mL/min. The washing solution was collected after 0.5, 2.5, and 8.5 h. The content of LE in the washing solution was quantified using HPLC (Shimadzu SIL-40C XR).

In Vivo Study: Male and female mice (C57BL/6, aged 8–10 weeks) were obtained from the Charles River Laboratories, Wilmington, MA. All the experiments conducted for this study were approved by the Schepens Eye Research Institute Animal Care and Use Committee (animal protocol number: 2021N000158). All animals were treated according to the tenets of the ARVO Statement for the Use of Animals in Ophthalmic and Vision Research. Each animal was deeply anesthetized with an intramuscular injection of 3 to 4 mg of ketamine and 0.1 mg of xylazine before all surgical procedures.

In Vivo Biocompatibility: Naïve (normal) mice (n=3) received a daily drop of PBA-MC eyedrops for 7 consecutive days and were monitored for signs of tearing, discharge, or other symptoms indicative of ocular discomfort or infection. Observations were documented daily, with slit lamp photographs taken on days 0, 1, 2, 4, and 7. To evaluate potential epithelial defects, 1 μ L of 2.5 % fluorescein (Sigma-Aldrich) was applied to the lateral conjunctival sac of unanesthetized mice using a micropipette. After 3 min, fluorescein staining was assessed under

cobalt blue light using slit lamp biomicroscopy equipped with a Topcon DC-4 digital camera attachment (SL-DC4) on day 7. Naïve mice (normal) served as controls. After 7 days, all mice were euthanized, and their eyes were preserved in 4 % paraformaldehyde for further histological analysis.

In Vivo Assessment of Corneal Retention Time: To prepare PBA-MC-LE evedrops for the *in vivo* study, the PBA-MC-LE solution was first concentrated using a protein concentrator (MWCO 20 kDa) to achieve an LE concentration of 5 % (w/v). The concentrated solution was then diluted with the matrix to reach a final LE concentration of 0.5 % (w/v). To evaluate the corneal retention time, a single drop (3 μL) of the PBA-MC-LE or commercial LE eyedrops (Oceanside®, 0.5 % LE Ophthalmic Suspension) was applied to the eyes of an esthetized mice (n = 5 per group) based on a previously developed protocol [48]. Manual eye blinking was performed every 30 s. Anterior segment optical coherence tomography (AS-OCT), Bioptigen Spectral Domain Ophthalmic Imaging System Envisu R2200 with 12-mm telecentric lens (Bioptigen Inc, Durham, NC, USA) imaging, was conducted at baseline (before instillation) and at multiple time points after instillation and manual eve blinking. The area above the corneal surface occupied by the evedrops was identified in each AS-OCT image, quantified using ImageJ, and plotted against the number of manual eye blinks. The area under the curve (AUC_{0-last}) was then calculated using GraphPad Prism 10.3.1.

Ocular Drug Flux in Naïve Mice: The mice received one drop (\sim 5 μL) of either PBA-MC-LE eyedrop formulation or commercial LE eyedrops (Oceanside®, 0.5 % LE Ophthalmic Suspension). After the drops were administered, the mice (n=3–4 mice per time point per group) were euthanized after 1 h and 24 h. Corneal tissues were collected, weighed, and stored at -80 °C prior to analysis. The mice were re-dosed with eyedrops at each time point. Corneal tissue samples were homogenized and extracted with a mixture of acetonitrile/water (1:1 (v/v)) before analysis [49]. Drug concentrations in the tissues were quantified using Liquid Chromatography-Mass Spectrometry (LC-MS, Agilent 1260 Infinity II).

Electrocauterization of the Corneal Surface: Mice were anesthetized and placed under the operating microscope. Using the tip of a hand-held electrocautery, four burns were applied to the central 50 % of the cornea of the right eye [49]. Immediately after surgery, triple antibiotic ophthalmic ointment was applied to the ocular surface. Mice started receiving treatment on day 0. The treatment groups were divided into 3 subgroups (n = 12/subgroup): i) no treatment, ii) commercial 0.5 % LE ophthalmic solution (Oceanside®, 0.5 % LE Ophthalmic Suspension) 4x/day, and iii) our PBA-MC-LE eyedrop formulation 1x/day. All experiments were performed randomly while maintaining an equal number of male and female mice within each group and its subgroups. On day 7, all animals were sacrificed and their corneas were excised for quantitative reverse transcription polymerase chain reaction(qRT-PCR) and immunohistochemistry (IHC) analysis.

Anterior Segment Optical Coherence Tomography (AS-OCT): Anterior segment images were taken using AS-OCT on days 0, 2, 4, and 7 after injury. AS-OCT was performed under general anesthesia. Central corneal thickness was measured using the AS-OCT built-in software.

Slit Lamp Biomicroscopy: Slit lamp biomicroscopy was performed on days 0, 2, 4, and 7. ImageJ was used to quantify the opacity area and total corneal area. The percentage of opacity area (% per cornea) was obtained by dividing the opacity area by the total corneal area.

RNA Isolation and qRT-PCR Analysis: Corneal tissues were harvested under a dissecting microscope and placed in TRIzol solution (15,596,026, Invitrogen). Total RNA from corneas was extracted using the RNeasy Mini Kit (QIAGEN, Hilden, Germany) according to the manufacturer's instructions and quantified using a spectrophotometer (NanoDrop 2000; Thermo Fisher Scientific, Waltham, MA, USA). Complementary DNA (cDNA) was synthesized from RNA using the QIAGEN QuantiTect Reverse Transcription Kit according to the manufacturer's instructions. qRT-PCR was performed using TaqMan Universal PCR Master Mix (Thermo Fisher Scientific) reagents and Eppendorf

Mastercycler Ep gradient Instrument. The primers for IL-1 β , IL-6, and glyceraldehyde-3-phosphate dehydrogenase (GAPDH) were Mm00434228_m1, Mm00446190_m1, and Mm99999915_g1 (Thermo Fisher Scientific), respectively. GAPDH served as the internal reference gene.

Histopathological Analysis and Immunohistochemistry Staining: The entire eyes were harvested from mice fixed in 4 % paraformaldehyde and subsequently embedded in paraffin and sectioned. For hematoxylin and eosin (H&E) staining, the sections from each group were deparaffinized, stained with Mayer's hematoxylin, and counterstained with alcoholic eosin to evaluate the corneal thickness and the integrity of ocular structures. For CD45⁺ staining, the sections were deparaffinized and blocked in 5 % BSA. The slides were then incubated with mouse CD45⁺ Antibody (Catalog # AF11, Biotechne) diluted in 5 % BSA for 2 h at 4 °C. After washing with tris buffered saline (TBS, Bio-RAD), the slides were incubated with Donkey anti-Goat IgG (H+L) Highly Cross-Adsorbed Secondary Antibody, Alexa FluorTM Plus 488 secondary antibodies (Thermo Fisher) diluted in 5 % BSA for 1 h. The slides were washed three times, and the staining was mounted with Vectashield with DAPI and examined using Nikon Eclipse E800 microscope.

Statistical Analysis: Statistical analysis was conducted using one- or two-way ANOVA tests with GraphPad Prism 8.4.3 software. Each experiment involved a minimum of three samples. The data are expressed as means \pm standard deviation, and significance levels are denoted as follows: *p < 0.05, **p < 0.01, ***p < 0.001, ****p < 0.0001.

3. Results and discussion

To address the problems associated with conventional eyedrops, including poor drug retention on the cornea, low drug bioavailability, and the need for frequent application, we developed a mucoadhesive micellar eyedrop solution. This formulation can enable sustained delivery of anti-inflammatory drugs to cornea without requiring multiple applications. An amphiphilic block copolymer with a PBA end group, PBA-PEG-b-p(HPMA-Lac_m), was synthesized via a free radical polymerization to enhance the mucoadhesion of MCs formed by the copolymer. This copolymer consisted of a hydrophilic PEG block with stealth properties [50] which formed the micellar shell, and a hydrophobic HPMA block with oligolactide (Lac_m) moieties, serving as a host for encapsulating hydrophobic LE (Fig. 1A). LE was loaded into the core of MCs using a self-assembly method by evaporating the organic solvent. The PBA groups on LE-loaded PBA-MC facilitated mucoadhesion by covalent conjugation to the sialic acid groups present in mucin (Fig. 1B). Moreover, the mucoadhesion characteristic of PBA-MC was improved by dispersing these MCs within a shear-thinning matrix with an appropriate viscosity (Fig. 1C).

3.1. Synthesis and characterization of PBA-PEG-b-(HPMA-Lac $_m$) copolymer

Frequently utilized mucoadhesive moieties include mussel-inspired motifs such as catechol [51], PBA [32,33], maleimide [52–54], and thiol groups [55,56]. Maleimide is susceptible to degradation during multi-step synthesis, necessitating the use of protective groups to maintain its stability [57]. Thiol groups, on the other hand, are susceptible to oxidation, and their conjugation with targets is often reversible, leading to reduced adhesion strength [58]. Incorporating catechol at high conjugation efficiency can be challenging as it can easily undergo auto-oxidation to form highly reactive quinones and polymerize into oligomers [59]. In contrast, PBA forms stable boronic esters through covalent bonding with compounds containing cis-diol groups [32,33], such as polysaccharides, glycoproteins, and glycolipids which remain intact at physiological pH [34]. This unique interaction has propelled PBA into the spotlight for ocular applications, as it can engage with diol groups of glycoproteins and glycolipids on corneal

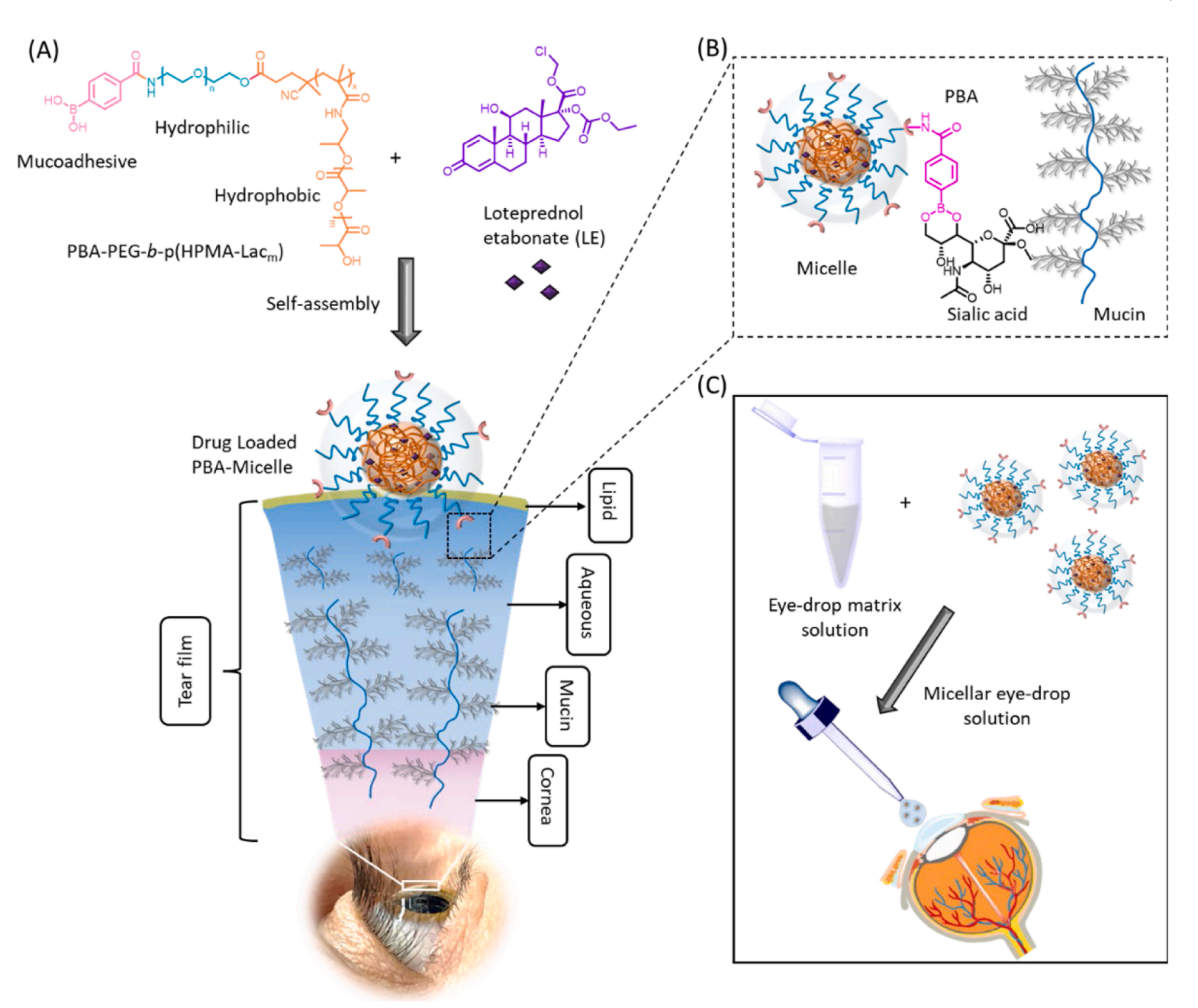


Fig. 1. Schematic illustration of mucoadhesive micellar eyedrop solution. (A) Formation of LE loaded MCs through self-assembly of PBA-PEG-b-p(HPMA-Lac_m) copolymer in a buffer solution; (B) schematic representation of the interaction between LE loaded PBA-MC and sialic acid groups present on the ocular surface mucin; and (C) formation of eyedrop solution containing mucoadhesive drug loaded MCs.

mucin [16,60]. Therefore, we synthesized a block copolymer with a PBA end group to develop a mucoadhesive micellar eyedrop formulation.

3.1.1. Synthesis and characterization of PBA-PEG-OH

To engineer PBA-PEG-b-(HPMA-Lac_m) copolymer, PBA was first conjugated with hydroxyl-PEG-amine (HO-PEG-NH₂) using aEDC/NHS reaction to form PBA-PEG-OH (Fig.S1-A). To increase efficiency of PBA conjugation to HO-PEG-NH2, we adjusted some parameters including solvent type, activation pH, and temperature, as summarized in **Table S2.** The conjugation efficiency was calculated as \sim 36.0 % based on ¹H NMR analysis, with activation pH set to 4.5, by using 2-(N-morpholino) ethanesulfonic acid (MES) buffer, and the temperature set to 60 °C (Fig. S1-Bi). EDC/NHS activation is well-suited for various aminebearing systems, with the optimal pH often falling into the range of 5–6 [61,62]. Therefore, we adjusted the MES buffer pH = 6 to further improve PBA conjugation. Switching to a less acidic buffer improved the conjugation efficiency to ~44.8 % calculated from the ¹H NMR spectra (Fig. S1-Bii). Even though we increased conjugation efficiency, we found that pH was not the sole factor affecting conjugation efficiency. The formation of the NHS-ester intermediate is crucial for facilitating the conjugation between carboxylic acid and amine due to its high reactivity. However, high temperatures (> 50 $^{\circ}$ C) favor NHS-ester hydrolysis instead of reacting with the amine [63]. Therefore, we reduced the activation temperature to 45 $^{\circ}\text{C}$ while keeping the pH = 6. DMSO was also used as co-solvent to prevent PBA precipitation at 45 °C in MES buffer. With these conditions, the PBA conjugation efficiency improved

to 77.8 % (Fig. S1B-iii and Table S2). To the best of our knowledge, this is the first report on achieving such a high level of conjugation efficiency of PBA to NPs for ocular drug delivery.

3.1.2. Synthesis of PBA-PEG-ACVA macroinitiator

The PBA-PEG-OH was then conjugated with ACVA initiator via a DCC/DMAP coupling reaction to obtain hydrophilic macroinitiator PBA-PEG-ACVA (Fig. 2A, step 1). PBA-PEG-ACVA macroinitiator was characterized by 1 H NMR spectroscopy, which showed characteristic signals of PBA at 7.91 and 7.80 ppm and protons next to the ester oxygen at 4.26 ppm along with protons in PEG repeating unit (-C H_2 C H_2 O-) between 3.44 – 3.84 ppm (Fig. 2B).

3.1.3. Synthesis and characterization of HPMA-Lac_m monomer

After we successfully synthesized a hydrophilic macroinitiator PBA-PEG-ACVA, a fully degradable hydrophobic HPMA-Lac $_{\rm m}$ monomer was obtained via a ring-opening polymerization (ROP) between HPMA monomer and L-lactide (Lac) catalyzed by tin octoate (Sn(Oct) $_2$) as previously reported [41]. The purity of the HPMA-Lac $_{\rm m}$ monomer was verified by 1 H NMR spectroscopy, revealing the vinyl protons at 5.69 and 5.33 ppm, while the methyl group of Lac repeating unit appeared between 1.4 – 1.6 ppm (Fig. S2). The average Lac repeating units (m) were calculated using the integration ratio between the repeating Lac units and the vinyl protons of HPMA-Lac $_{\rm m}$ monomer, resulting in m=6.

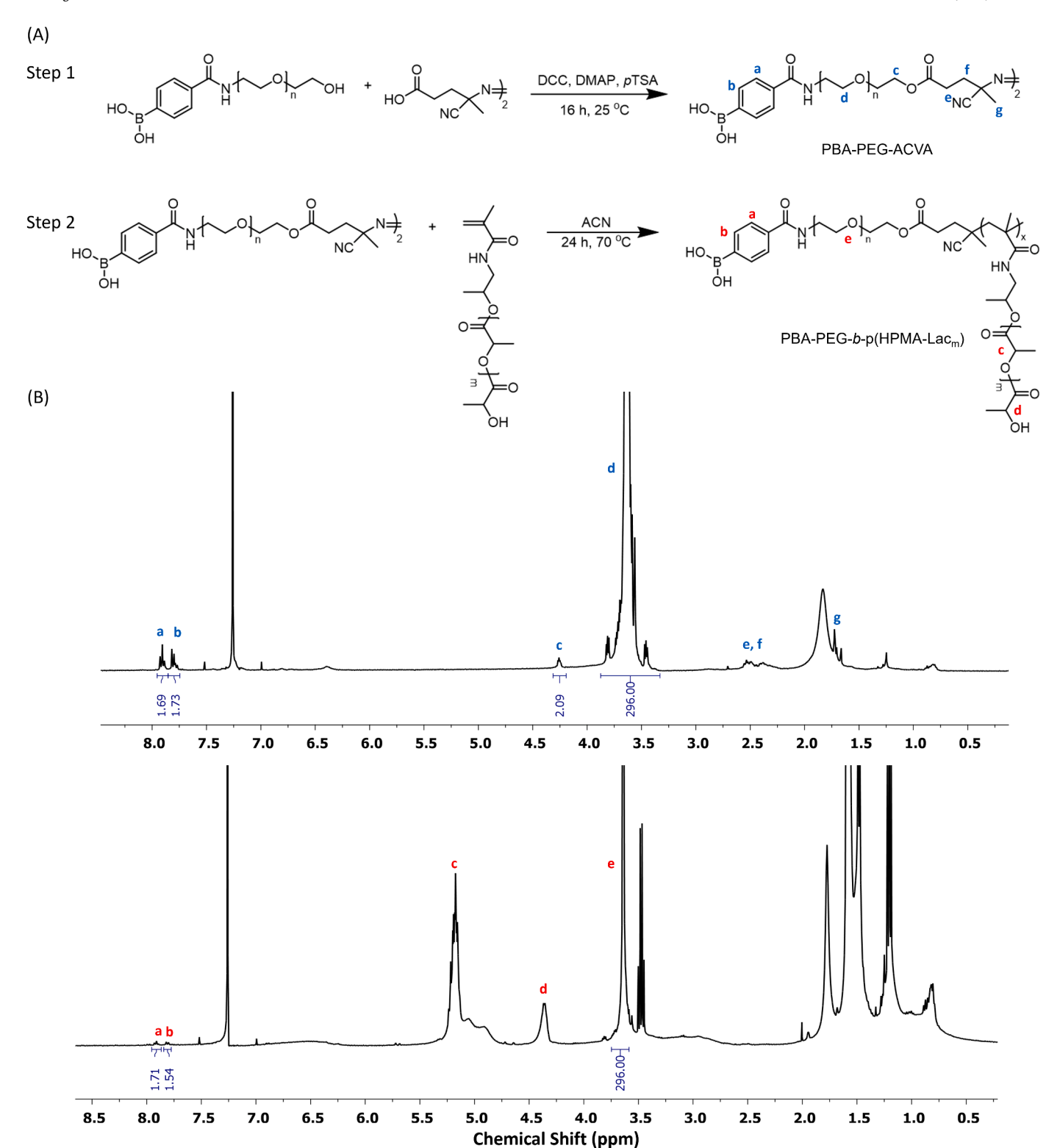


Fig. 2. Synthesis of PEG-b-(HPMA-Lac_m) copolymer with PBA end groups. (A) Synthesis of PBA-PEG-ACVA macroinitiator through DCC/DMAP coupling and the formation of the block copolymer PBA-PEG-b-p(HPMA-Lac_m) via free radical polymerization; ¹H NMR characterization of (B) PBA-PEG-ACVA macroinitiator; and (C) PBA-PEG-b-p(HPMA-Lac_m) copolymer in CDCl₃.

3.1.4. Synthesis of PBA-PEG-b-p(HPMA-Lac_m) copolymer

A free radical polymerization of HPMA-Lac $_{\rm m}$ monomer was initiated by PBA-PEG-ACVA macroinitiator to yield amphiphilic block copolymer, PBA-PEG-b-p(HPMA-Lac $_{\rm m}$) (Fig. 2A, step 2). The polymerization was carried out in anhydrous ACN for 24 h at 70 °C. The synthesis of PBA-PEG-b-p(HPMA-Lac $_{\rm m}$) block copolymers was confirmed by $^{\rm 1}$ H NMR

analysis in CDCl $_3$ (Fig. 2C). Typical peaks of PEG repeating unit and Lac repeating unit of HPMA-Lac $_m$ appeared between 3.44 – 3.84 ppm and 5.12 – 5.26 ppm, respectively. PBA groups on the copolymer chain end after the polymerization were clearly observed at 7.92 and 7.81 ppm (Fig. 2C). The ratio of PBA groups bound to the copolymer chain end was calculated by integration ratio between PBA and PEG repeating unit

protons, indicating that 81.3 % of copolymer chains contained PBA at the chain end. The number of hydrophobic blocks (x) in PBA-PEG-b-p (HPMA-Lac $_m$) block copolymer was determined by the integration ratio between the protons at the tail of the HPMA-Lac $_m$ monomer and protons in the PEG repeating units, resulting in 37 (Eq. (3), Materials and Methods). The average molecular weight of the copolymer (Mw-cop) was calculated using Eq. (4), Materials and Methods and found to be 22,591.9 g/mol.

As a control group, we also synthesized a block copolymer using HPMA-Lac $_{\rm m}$ monomer and PEG-ACVA macroinitiator devoid of PBA groups based on the procedure explained previously [42]. Initially, PEG-ACVA macroinitiator was synthesized according to previously published method [64]. The 1 H NMR spectrum of PEG-ACVA showed characteristic signals of protons adjacent to the ester oxygen at 4.26 ppm, while it exhibited the PEG repeating unit (-CH $_{2}$ CH $_{2}$ O-) between 3.44 - 3.84 ppm (Fig. S3). After characterization of PEG-ACVA, the

polymerization was carried out in anhydrous ACN at 70 $^{\circ}$ C for 24 h in the presence of the HPMA-Lac_m monomer, and the obtained copolymer (PEG-b-p(HPMA-Lac_m)) was characterized by 1 H NMR spectroscopy. 1 H NMR showed peaks of the PEG repeating unit between 3.44 – 3.84 ppm and the Lac repeating unit of HPMA-Lac_m between 5.12 – 5.26 ppm (**Fig. S4**). This PEG-b-p(HPMA-Lac_m) copolymer without PBA was utilized to engineer MCs used as control group.

3.2. Preparation and characterization of MCs

The copolymers, with and without PBA end groups, were self-assembled into MCs using a solvent evaporation method (Fig. 1A). Initially, PBA-PEG-b-p(HPMA-Lac_m) or PEG-b-p(HPMA-Lac_m) copolymers were dissolved in acetone at a concentration of 10 mg/mL solution. Subsequently, this copolymer solution was added dropwise into an AAB solution (120 mM, pH = 5), while stirring with a magnetic

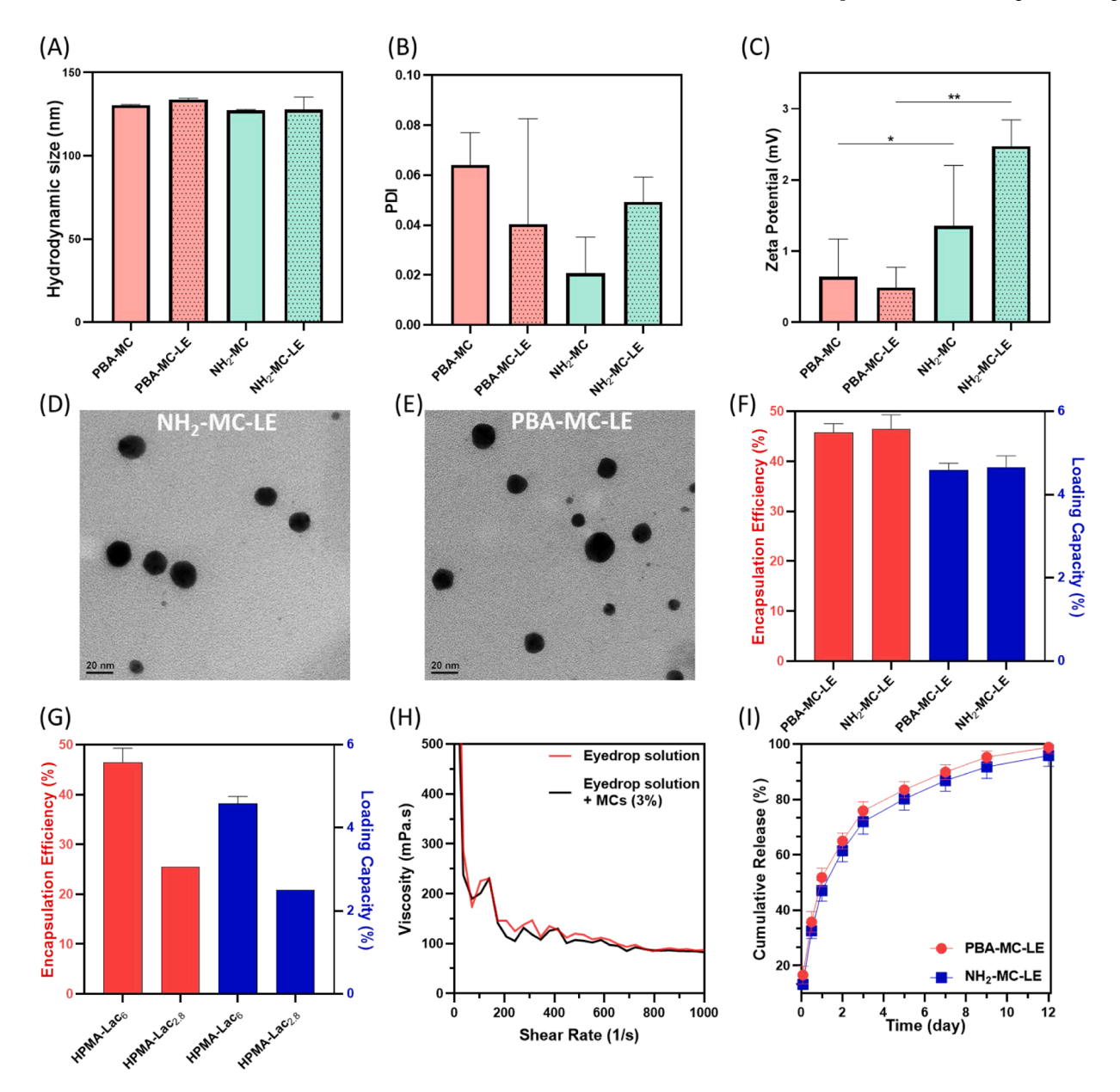


Fig. 3. Characterization of MCs and *in vitro* release studies. (A) Hydrodynamic size measurements, (B) PDI, and (C) surface zeta potential measurements of LE loaded MCs (NH₂-MC-LE, PBA-MC-LE) and unloaded MCs (NH₂-MC, PBA-MC); representative TEM images of (D) NH₂-MC-LE and (E) PBA-MC-LE; (F) encapsulation efficiency (EE %) and drug loading capacity (LC %) of MCs formed with copolymer/LE ratio 10:1; (G) comparison of EE % and LC % of PBA-MC formed with 6 Lac repeating unit as compared to lower Lac repeating unit (\sim 2.8); (H) rheology studies of eyedrop solution and eyedrop solution mixed with 3 % (w/v) PBA-MC; (I) *in vitro* release of LE from PBA-MC-LE and NH₂-MC-LE eyedrops at 37 °C in an artificial tear solution containing 2 % (v/v) Triton X-100.

stirrer. As acetone evaporated, the copolymers self-assembled into MC structures, with the hydrophilic PEG block directing toward water and the hydrophobic block p(HPMA-Lac $_{\rm m}$) aggregating to reduce interactions with water. The hydrophobic core of MCs, composed of HPMA-Lac $_{\rm m}$, would enable to encapsulate a variety of hydrophobic drugs [65–67]. Herein, we encapsulated an anti-inflammatory drug, LE, within the hydrophobic core of MCs formed by PBA-PEG-b-p(HPMA-Lac $_{\rm m}$) and PEG-b-p(HPMA-Lac $_{\rm m}$) copolymers. The drug loaded MC formulations were prepared by an additional step involving dissolution of LE in DMSO and mixing this solution with the copolymer solution.

The hydrodynamic sizes of drug loaded and unloaded MCs were measured via DLS. The hydrodynamic sizes of drug loaded MCs (PBA-MC-LE) and unloaded MCs (PBA-MC), formed by PBA-PEG-b-p(HPMA-Lac_m) copolymers, were found as 133.8 \pm 0.8 nm with a polydispersity index (PDI) of 0.04 and 130.6 \pm 0.3 nm with a PDI of 0.06, respectively. Similarly, we measured the hydrodynamic sizes of drug loaded and unloaded MCs formed by PEG-b-p(HPMA-Lac_m) copolymer without PBA named as NH2-MC-LE and NH2-MC, respectively (used as control groups). The sizes of drug loaded MCs (NH2-MC-LE) and unloaded MCs (NH₂-MC) were measured to be as 127.8 \pm 8.1 nm with a PDI of 0.05, and 127.4 \pm 0.5 nm with a PDI of 0.02, respectively (Figs. 3A, B). No significant difference was observed in size between unloaded and LE loaded MCs in both PBA and control groups. The low PDIs in this study indicated a high level of homogeneity in the size of the MCs. The surface charge of the MCs was determined using a Zetasizer. Zeta potentials of MCs were found as 0.5 \pm 0.3 mV, 0.6 \pm 0.6 mV, 2.5 \pm 0.4 mV, 1.4 \pm 1.0 mV for PBA-MC-LE, PBA-MC, NH2-MC-LE and NH2-MC, respectively (Fig. 3C). Also, the morphology of PBA-MC-LE and NH₂-MC-LE was evaluated by TEM (Figs. 3D, E). The average sizes of dry micellar structures were found to be around 20 nm, based on TEM images, for PBA-MC-LE and NH2-MC-LE. This was attributed to the hydrophilic PEG shell, which can retain a large amount of water in the solution. However, the water portion was depleted during the drying process, leading to the observed size reduction in the dried micellar structures [68.69].

CMC is an important parameter for evaluating MC performance for drug delivery applications. A lower CMC indicates that MCs form at lower concentrations, which is beneficial for stability and effectiveness in ocular drug delivery. MCs with a low CMC are stable at concentrations suitable for use in the eye, reducing the risk of rapid dispersion and irritation [70]. The CMC was measured using a well-established pyrene fluorescence probe method [43,44]. Pyrene, a hydrophobic fluorescent molecule, has an excitation spectrum that is highly sensitive to environmental polarity. As MCs form, pyrene partitions into the hydrophobic MC core, leading to an increase in the I338/I333 intensity ratio. Plotting this ratio against polymer concentration generates a sigmoidal curve, with the inflection point corresponding to the CMC. As shown in Fig. S5, the CMC value of the engineered PBA-MC was determined to be 0.05 mg/mL, which remained consistent in both media, with no significant shift in the inflection point. This low CMC suggested that MC formation occurred at relatively low concentrations [71], which is beneficial for ophthalmic applications. Moreover, the consistency in CMC across different media indicates that the formation of MC is robust, unaffected by variations in pH, ionic strength, or composition.

The amount of LE loaded inside MCs hydrophobic core can be easily regulated by changing copolymer/drug ratio. In our previous work on engineering a drug eluting adhesive patch, we showed that the EE % of LE in PEG-b-p(HPMA-Lac $_{\rm m}$) MCs increased as the copolymer/LE ratio decreased. However, no significant differences were observed among groups with a copolymer/LE ratio lower than 10:1 [12]. Based on these findings, copolymer/LE ratio of 10:1 was selected for the in vitro loading and release experiments in this work. The drug EE % and LC % were determined by HPLC, using a calibration curve of LE at five different concentrations. The EE % was found to be 45.8 \pm 2.0 % for PBA-MC-LE and 46.5 \pm 3.2 % for NH₂-MC-LE at a 10:1 copolymer/LE ratio (Fig. 3F). Furthermore, LC % of MCs was calculated as 4.6 \pm 0.2 % for PBA-MC-LE

and 4.7 \pm 0.3 % for NH₂-MC-LE (Fig. 3F). These results indicated a nearly 2-fold increase in both EE % and LC % compared to our previous work, where EE % and LC % were 25.5 % and 2.5 % at a 10:1 polymer/drug ratio, respectively (Fig. 3G) [12]. The substantial enhancement in EE % and LC % is attributed to the higher number of Lac repeating groups in the HPMA-Lac₆ monomer, in contrast to our previous study that utilized a mixture of HPMA-Lac₂, HPMA-Lac₃ and HPMA-Lac₄ (average Lac \sim 2.8) [12]. In this study, during the synthesis of the copolymer, a higher molar ratio of monomer: macroinitiator (200:1) was applied to increase the hydrophobic portion of the copolymer, which contributed to higher encapsulation efficacy of the non-polar drug [42].

In vitro drug release profiles for PBA-MC-LE and NH2-MC-LE in an eyedrop solution were obtained via a dialysis method under sink conditions using an artificial tear solution as the release medium at pH = 7.4. The eyedrop solution was made of HA, glycerin, hypromellose, water, benzalkonium chloride (as a preservative), and buffering systems based on the ophthalmic formulations [72-74]. HA can provide desirable viscosity, shear thinning behavior, and lubrication. HA's viscosity decreases under shear stress, such as when applied to the ocular surface, allowing the solution to flow easily upon application. Once on the surface, however, the viscosity increases, which helps reduce tear drainage and promotes longer contact time with the ocular surface [76]. Glycerin helps to reduce surface tension and hypromellose provides mucoadhesion, which can extend the retention time of the eyedrop on the cornea, allowing the targeting moieties to form interaction with the corneal mucin [74]. Therefore, we first evaluated the shear thinning behavior of eyedrop solution with and without MCs by rheology studies. As is shown in Fig. 3H, the formulated eyedrop solution showed desirable shear thinning behavior and proper viscosity (~80 mPa·s), ensuring long-term precorneal retention time. The addition of MCs did not influence the rheological properties of the eyedrop solution, ensuring its clinical use in practice.

After characterization of the eyedrop solution, the MCs were dispersed in 1 mL of this solution and dialyzed against 10 mL of artificial tear fluid. In order to increase the solubility of LE in an artificial tear solution, we added 2 % (v/v) non-ionic surfactant Triton X-100 to the solution. During the period of release study, 2 mL of artificial tear solution was sampled at each time point, and an equal volume of fresh artificial tear solution was added to maintain a constant total volume. At predetermined time intervals, the concentration of released LE was determined by HPLC. Similar to other drug delivery nanocarriers, PBA-MC-LE eyedrops showed a two-phase release profile including an initial burst release phase (35.8 \pm 4.2 % at 12 h, 51.9 \pm 3.9 % at 24 h) followed by a slow, non-linear release of 100 % after 12 days. Similarly, NH2-MC-LE released 32.6 \pm 3.2 %, 47.1 \pm 3.9 %, and 95.9 \pm 4.4 % of LE after 12 h, 24 h, and 12 days, respectively. Modifying the surface of MCs with PBA did not affect the release profile of LE (Fig. 3I). In our study, the engineered drug loaded MCs completely released their payload after 12 days due to the hydrolysis of lactate chains of copolymers. In another study utilizing PBA-chitosan oligosaccharidevitamin E, 75 % of the encapsulated coumarin-6 was released from the MCs after only 30 min, and almost all drug payload was released after 2 h [33]. However, our PBA-MC-LE eyedrops demonstrated lower release rates, especially during the first few hours and the first day. This slower release profile plays a pivotal role in ensuring a sustained anti-inflammatory effect, thus allowing for a significant reduction in dosage to attain the desired therapeutic outcome. Moreover, minimizing burst release can mitigate the risk of adverse effects associated with high initial doses. In the case of anti-inflammatory drugs like corticosteroids, minimizing burst release is particularly important because it can help reduce various side effects including pain, increased intraocular pressure, delayed corneal wound healing and the possibility of systemic absorption [75].

The observed sustained release over 12 days in vitro, despite the 45 % encapsulation efficiency, suggests that the system still provided

controlled and prolonged drug release, which is crucial for effective ocular drug delivery. Importantly, the MCs could be easily concentrated to ensure an adequate drug dosage for ocular applications using a protein concentrator (MWCO 20 kDa). This flexibility allowed us to adjust the micellar formulation as needed to meet the desired drug concentration, further enhancing the therapeutic potential of the system.

While our formulation demonstrated sustained drug release for up to 12 days *in vitro*, we recognize that this does not directly reflect ocular residence time *in vivo*. Although the MCs are designed to interact with mucins via dynamic covalent bonding, the ocular mucin layer undergoes relatively rapid turnover due to blinking and tear clearance [76]. As such, the *in vivo* retention of the formulation is expected to be limited by this biological process. These findings suggest that while mucin binding may enhance initial retention and bioavailability, repeated administration may still be necessary for long-term therapeutic efficacy. In light of this, a once-daily dosing regimen of the PBA-MC-LE eyedrop formulation was employed in the proof-of-concept *in vivo* efficacy study (Section 3.6).

3.3. In vitro and ex vivo mucoadhesion studies

Mucoadhesive MCs, when interacting with mucin, exhibit a tendency to entangle and aggregate, resulting in the formation of larger, irregularly shaped granules. This aggregation scatters visible light and reduces the transparency of the solution [77]. To assess mucoadhesive strength of MCs, we measured the turbidity of mucin solutions using ultraviolet-visible (UV-vis) spectroscopy at 600 nm of optical density (OD) after mixing with MCs solution. At a 0.1 ratio of MCs to mucin, PBA-MC, NH2-MC, and DPBS (no MCs) groups exhibited no significant differences. However, when mucin solution was mixed with PBA-MC and NH2-MC at and above 1 MCs/mucin ratios (1, 2, 3, 10), there was an increase in turbidity as the weight ratio of MCs increased (Fig. 4A). This observation suggested that both the PBA groups on PBA-MC and the amine group on NH₂-MC possessed mucoadhesive properties [78]. The amine end group bears a positive charge at pH < 9, enabling it to interact with mucin through ionic interaction, which is negatively charged due to carboxyl groups and sulfate groups. However, at MCs/mucin ratios of 1, 2, and 3, PBA-MC induced significantly higher (nearly two-fold) changes in turbidity compared to NH2-MC. This difference suggests a more pronounced mucoadhesive effect, attributed to the presence of PBA groups on the surface of MCs. At an MCs/mucin ratio of 10, PBA-MC led to a further increase in turbidity compared to samples at an MCs/mucin ratio of 3, but at a slower rate. This observation implies that a significant portion of the mucin in the solution interacted with PBA-MC, and there was insufficient free mucin to sustain the higher increasing trend. In contrast, the NH $_2$ -MC group did not exhibit a significant increase in turbidity at an MCs/mucin ratio of 10 compared to 3, indicating a limited mucoadhesive effect by amine groups alone (Fig. 4A).

Moreover, we explored the mucoadhesive properties of PBA-MC with sialic acid using a fluorescence spectrometer. Sialic acid, which is abundant in corneal mucin, was selected because PBA can covalently bind to its cis-diol groups [79]. PBA inherently exhibits fluorescence, but this fluorescence diminishes when PBA forms covalent bonds with diol groups. This phenomenon can be tracked using a fluorescence spectrometer to assess the binding of PBA and other diol species [80-82]. The emission of PBA-MC (50 µg/mL) was measured both before and after mixing with various concentrations of sialic acid in water (0, 0.02, 0.05, 0.1, 0.2, 0.5 mM) using a fluorescence spectrometer. As the concentration of sialic acid increased, the fluorescence emission intensity of the solution gradually decreased (Fig. 4B). These results demonstrate the PBA-MC could effectively bind to sialic acids within the mucin, presenting a promising platform for ocular drug delivery. This may address the challenges associated with the rapid clearance of NPs from the ocular surface.

To further evaluate the mucoadhesive properties of the PBA-MC on ocular surfaces, $ex\ vivo$ experiments were carried out using freshly isolated rabbit eyeballs. We evaluated the drug retention curve of LE loaded PBA-functionalized MCs containing 0.25 % (w/v) LE and compared it to commercial LE eyedrops (EYSUVIS®, 0.25 % (w/v)). In this experiment, fresh rabbit eyeballs were treated with 50 μ L of PBA-MC-LE or commercial LE eyedrops. After 15 min, the eyeballs were washed vertically with artificial tear fluid at a rate of 1 mL/min by using a syringe pump to mimic tear turnover [47,48]. The washing solution was collected after 0.5, 2.5, and 8.5 h. The content of LE in the washing solution was then quantified using HPLC. As shown in Fig. 4C, PBA-MC-LE showed a significantly higher drug retention rate (57.8 \pm 1.6 %) as compared with commercial LE (23.0 \pm 7.2 %) over 8.5 h, confirming their robust mucoadhesive properties.

3.4. In vitro biocompatibility studies and efficacy studies

To assess the biocompatibility of PBA-MC eyedrops, the viability and metabolic activity of PBA-MC treated human corneal epithelial cells were examined using Live/Dead and Actin/DAPI assays on days 1 and 5. The cells were exposed to a high concentration of PBA-MC (3 %) dispersed in the eyedrop solution added to the cultrue media, with untreated cells serving as the control. The Live/Dead assay results revealed

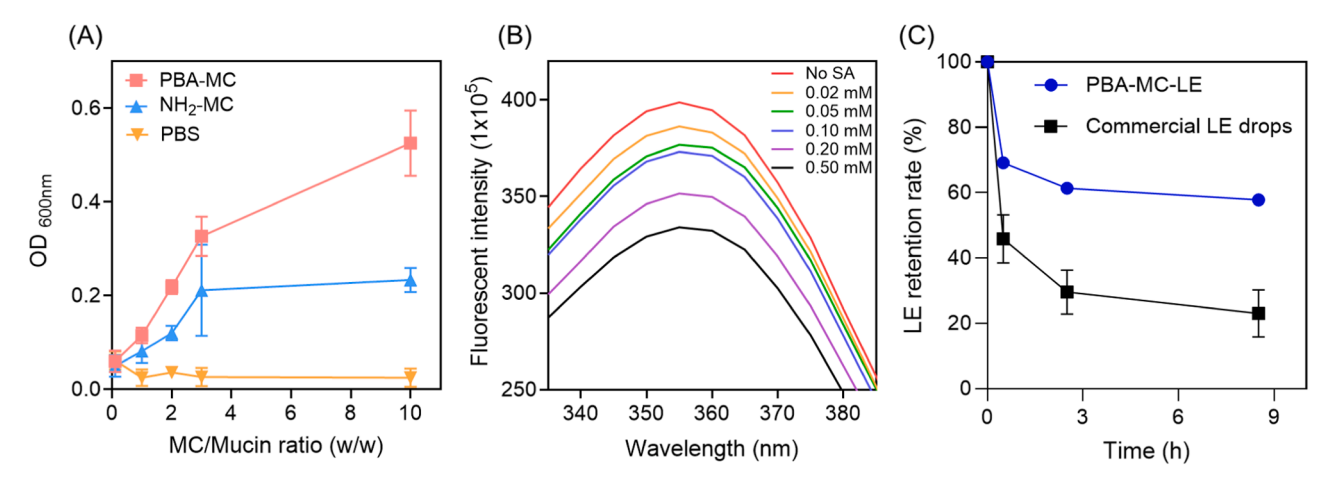


Fig. 4. *In vitro* and *ex vivo* mucoadhesion studies of MCs. (A) Turbidity measurements of PBA-MC and NH₂-MC mixed with mucin solution at different ratios (0.1, 1, 2, 3, and 10) and (B) fluorescence spectrometer measurement of PBA-MC dispersions mixed with different concentrations of sialic acid solution (0, 0.02, 0.05, 0.10, 0.20, and 0.50 mM). (C) The *ex vivo* drug retention rate of PBA-MC-LE (0.25 %) compared to commercial LE eyedrops (EYSUVIS®, 0.25 %), using isolated rabbit eyeballs.

a notable increase in cell numbers and high cell viability (>95 %) over 5 days. There was no significant difference observed between the PBA-MC eyedrops treated cells and untreated cells (Figs. 5A, B). Additionally, fluorescent Actin/DAPI staining of the cultured cells demonstrated the spreading and proliferation of cells on the culturing dish for both treated and untreated conditions, as indicated by the assembly of actin filaments in the cytoskeleton (Fig. 5C). Cell proliferation was further assessed using a PrestoBlue assay. Upon addition to the cells, PrestoBlue reagent undergoes modification in the reducing environment of healthy cells and changes color to red [83]. This color change can be detected using fluorescence measurements. As depicted in Fig. 5D, the metabolic activity of human corneal epithelial cells increased over 5 days for both groups, MC eyesdrops treated samples and the untreated group (control). These studies together confirmed the *in vitro* biocompatibility of the engineered mucoadhesive MCs.

To further investigate the possible effect of the matrix on inflammation, we performed an *in vitro* anti-inflammatory test using the RAW 264.7 macrophage cell line to assess the anti-inflammatory effects of each component [84]. Inflammation was induced with LPS, and CD80 staining was used to quantify the inflammatory response, as CD80 plays a key role in initiating and sustaining immune activation [45]. Six groups were evaluated: 1) Cell only (no treatment); 2) Cell + LPS; 3) Cell + LPS + PBA-MC; 4) Cell + LPS + PBA-MC-LE; 5) Cell + LPS + Matrix; and 6) Cell + LPS + PBA-MC-LE + Matrix. As shown in Fig. S6, the matrix, consisting of HA (0.5 %), glycerin (0.3 %), and hypromellose (0.3 %), did not show any significant anti-inflammatory effects.

Similarly, the PBA-MC vehicle alone did not yield any notable anti-inflammatory responses. These findings suggested that the therapeutic efficacy is primarily due to the LE component of the formulation. As discussed before, HA provides several beneficial properties, including biocompatibility, lubrication, and shear-thinning behavior [85], which make it an ideal component of the evedrop matrix. HA molecules share physical characteristics and composition similar to tear glycoproteins, allowing them to easily coat the corneal epithelium [86]. In addition to these advantages, the designed HA-based matrix contributes to the retention of the formulation by increasing its viscosity and promoting mucoadhesion to the corneal surface. Our matrix's mucoadhesion is primarily attributed to non-covalent interactions, such as hydrogen bond formation and interpolymer diffusion [87], enabling it to interact with the mucin layer on the ocular surface. However, these non-covalent interactions offer limited stability and strength at concentrations suitable for ophthalmic use [7,86,88]. To address this, the MCs are engineered for enhanced mucoadhesion through PBA functionalization. PBA can form stable cis-diol interactions with hydroxyl groups on mucosal glycoproteins at physiological pH, potentially improving MC retention on the ocular surface. Based on these combined mechanisms, we hypothesize that the synergy between matrix's non-covalent mucoadhesive interactions and the PBA-functionalized MCs' stable cis-diol bonding contributes to enhanced retention on the cornea. The existing commercialized matrix typically used for the LE alone is a standard aqueous solution, which lacks both the viscosity and the mucoadhesive properties provided by matrix and PBA. This difference in matrix

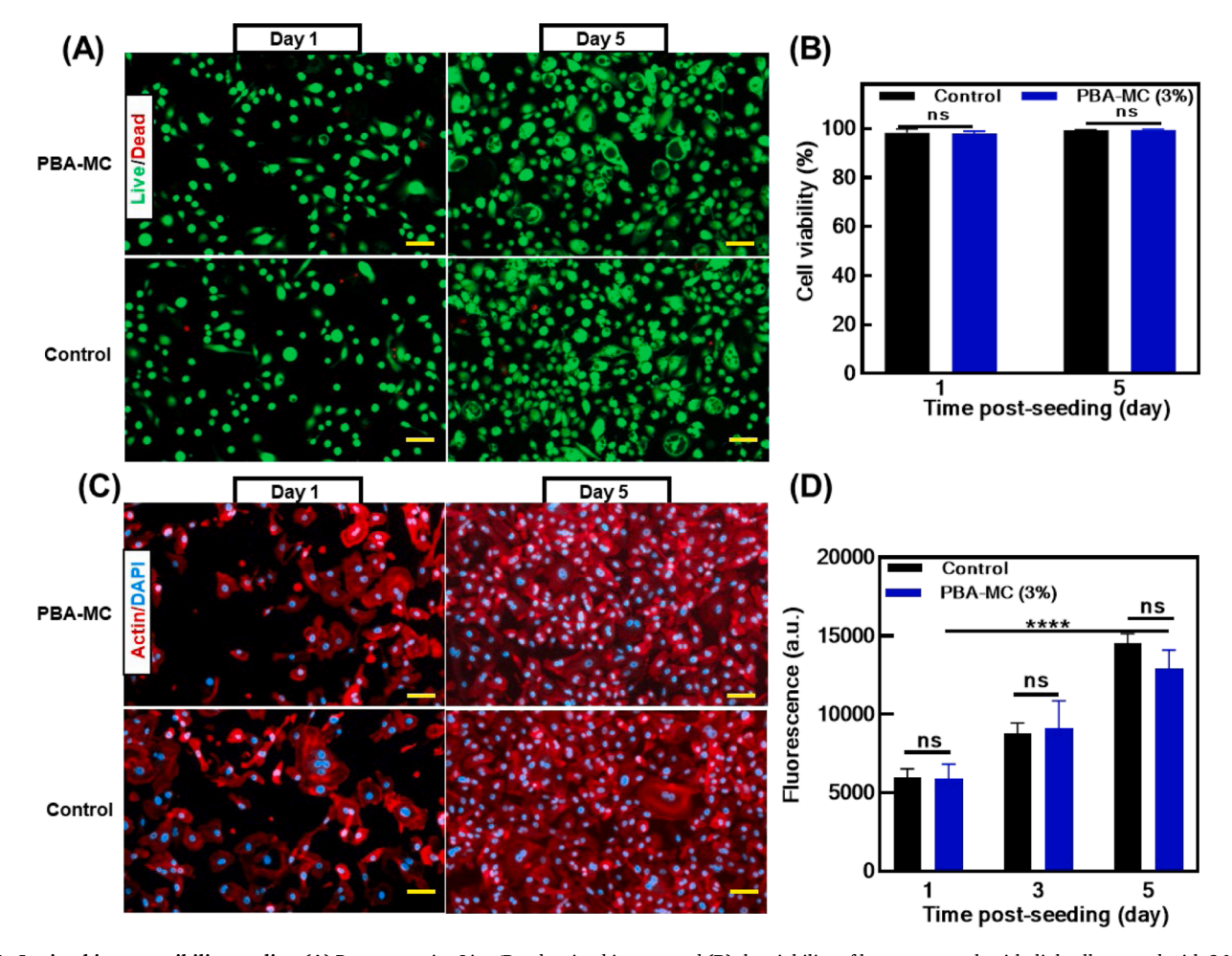


Fig. 5. In vitro biocompatibility studies. (A) Representative Live/Dead stained images and (B) the viability of human corneal epithelial cells treated with 3 % PBA-MC (in eyedrop solution) and untreated on days 1 and 5 (scale bars = $100 \mu m$); and (C) representative Actin/DAPI stained images from the human corneal epithelial cells treated with 3 % PBA-MC (in eyedrop solution) and untreated on days 1 and 5 (scale bars = $100 \mu m$); (D) quantitative analysis metabolic activity of PBA-MC eyedrops treated and untreated cells using a PrestoBlue assay at days 1, 3 and 5 post-seeding.

composition is expected to result in improved ocular retention and bioavailability with the MC-matrix formulation.

3.5. In vivo biocompatibility and corneal retention studies

To assess the biocompatibility of the topically applied PBA-MC eyedrops (PBA-MC dispersed in the matrix) under clinically relevant conditions, we employed a dosing regimen aligned with the intended

therapeutic use [89,90] (Section 3.6). Specifically, naïve mice (n=3) received PBA-MC eyedrops (1x/day) for 7 consecutive days. Clinical evaluations were performed daily using slit lamp biomicroscopy, which provides high-resolution assessments of the cornea and ocular surfaces. Slit lamp photographs were taken on days 0, 1, 2, 4, and 7. Additionally, fluorescein staining was performed after 7 days to assess any epithelial defects, and H&E staining was conducted on the eyes 7 days after treatment to assess corneal and retinal structures. Naïve (normal) mice

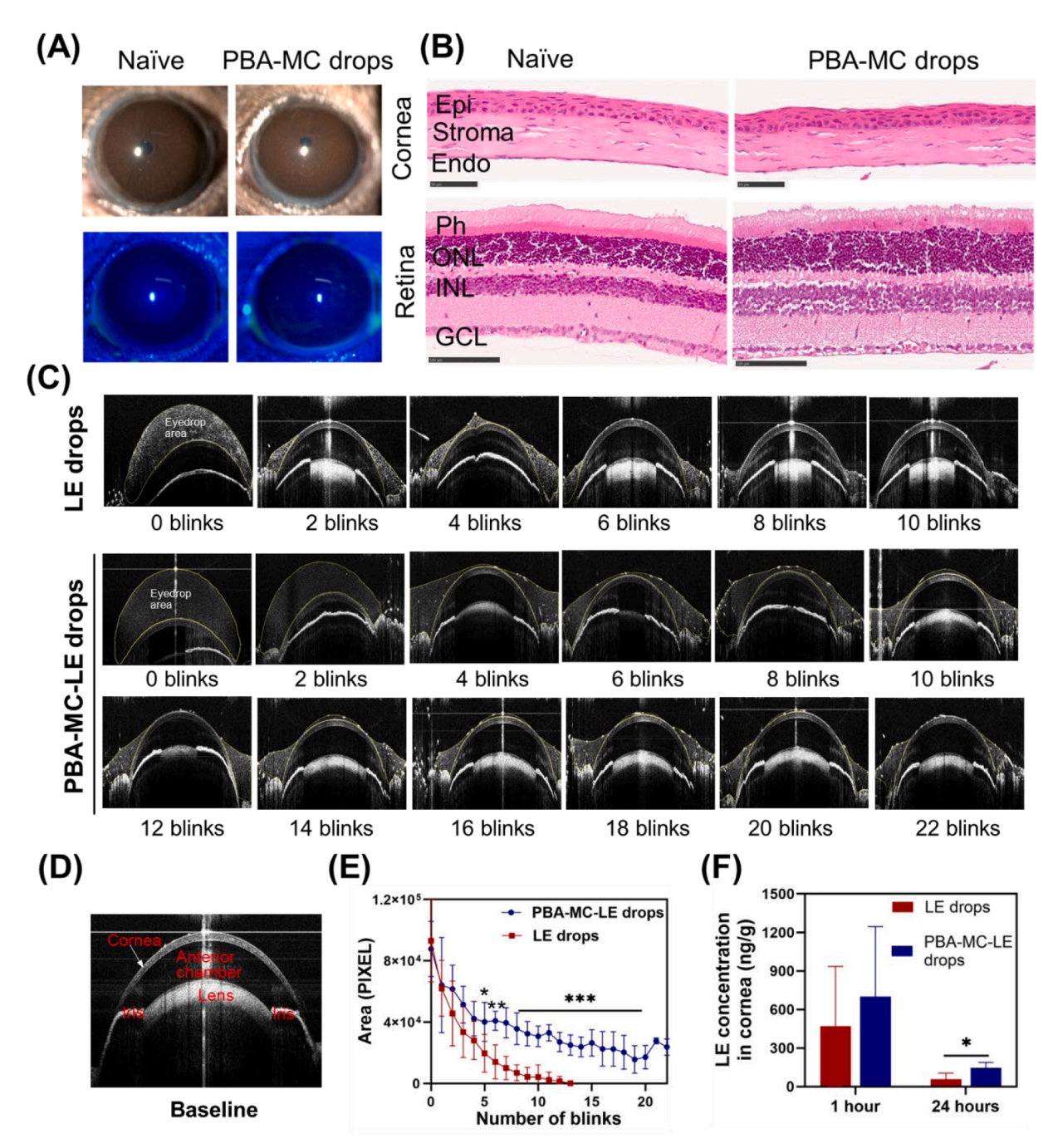


Fig. 6. *In vivo* biocompatibility of PBA-MC eyedrops and *in vivo* corneal retention and drug flux of PBA-MC-LE eyedrops. (A) Slit lamp bright field and cobalt blue light photographs of mouse eyes after 7-day topical treatment with PBA-MC eyedrops, compared to naïve mouse eyes. (B) Representative H&E stained images on day 7, showing intact corneal and retinal morphology of naïve and treated eyes (scale bars: cornea: $50 \, \mu m$, retina: $100 \, \mu m$). Corneal structures include the epithelium (Epi), stroma, and endothelium (Endo), while retinal layers include the photoreceptor layer (Ph), outer nuclear layer (ONL), inner nuclear layer (INL), and ganglion cell layer (GCL). The naïve cornea (normal) serves as a control. (C) Representative AS-OCT images of mouse eyes after applying one single drop of commercial LE or PBA-MC-LE eyedrops. Manual blinking of the murine eye was performed every $\sim 30 \, s$, and images were captured after each manual blink. (D) Representative AS-OCT images of a mouse eye at baseline (before eyedrop application). (E) Quantification of the area above the cornea occupied by the eyedrops by analysis of AS-OCT images. (F) Comparison of LE concentration in mouse corneas between PBA-MC-LE and commercial LE eyedrops. n = 3-5.

served as controls. Throughout the study, no adverse effects such as tearing, discharge, conjunctival redness, other symptoms of ocular discomfort, infection, or epithelial defects were observed (Figs. 6A and S7). The cornea and retina in the PBA-MC eyedrop group showed no detectable differences compared to normal eyes. H&E staining confirmed the integrity of corneal epithelium (Epi), stroma, or endothelium (Endo), with no signs of inflammatory cell infiltration (Fig. 6B). Moreover, retinal structures remained intact, showing well-preserved histological layers, including the photoreceptor layer (Ph), outer nuclear layer (ONL), inner nuclear layer (INL), and ganglion cell layer (GCL) (Fig. 6B). These results confirmed the *in vivo* safety of the once-daily administration of PBA-MC eyedrop formulation over a 7-day period. Future investigations will consider more frequent dosing regimens and prolonged treatment durations to characterize the safety profile comprehensively.

We evaluated the *in vivo* corneal retention and drug flux of the PBA-MC-LE eyedrop formulation. The corneal retention time of a single drop of the PBA-MC-LE eyedrop formulation against commercial LE eyedrops (Oceanside® Loteprednol Etabonate Ophthalmic Suspension, 0.5 %) was compared in mouse eyes (Figs. 6C-D). AS-OCT was used to monitor the reduction of eyedrop volume on the corneal surface over time and with repeated blinks [48]. After approximately 120 s (5 blinks), the AS-OCT images demonstrated a significantly larger area of PBA-MC-LE eyedrops remaining on the corneal surface compared to commercial LE drops (Figs. 6C-E). Further analysis showed that the AUC_{0-last} in the PBA-MC-LE eyedrop group was 2.71 times greater than commercial LE drops, indicating prolonged retention in the ocular surface (p < 0.0001). This enhanced retention is likely attributed to the improved mucoadhesion of the PBA-MC-LE eyedrops.

Additionally, we compared drug concentrations in the cornea of naı̈ve mice receiving a single drop of either PBA-MC-LE eyedrops or commercial LE drops. Drug levels were quantified using LC-MS. LE concentrations in the cornea were consistently higher in the PBA-MC-LE eyedrop group than in the commercial LE group at both 1- and 24 h post-application (Fig. 6F). Notably, after 24 h, the LE concentration in corneas treated with PBA-MC-LE eyedrops was 2.55 times higher (p=0.03) than in those treated with commercial LE eyedrops. These results suggested that PBA-MC-LE eyedrops prolonged drug retention on the ocular surface.

3.6. In vivo efficacy studies

In vivo efficacy of PBA-MC-LE evedrops (containing 0.5 % LE, 1X/ day) was evaluated using a mouse (C57BL/6) model of electrocauteryinduced corneal inflammation and was compared to commercial LE drops (0.5 %, 4X/day) and no treatment. Contralateral (non-injured) eve was also used as a control. The treatment started on day 0 and lasted for 7 days. The central corneal thickness (CCT) was measured via AS-OCT and corneal opacity was accessed by analysis of slit lamp photographs. AS-OCT images and slit lamp photographs demonstrated that injured eyes with no treatment progressively increased CCT, a measure of corneal edema, which can hinder vision by impairing transmission of light [91] (Figs. 7A, E, and S8) and developed corneal opacity after 7 days (Figs. 7B, F and S8). In contrast, treatment with commercial LE drops or PBA-MC-LE eyedrops drastically preserved CCT and prevented the loss of optical transparency. In vivo, by day 7, commercial LE drops (83 \pm 11 $\mu m)$ or PBA-MC-LE (83 \pm 7 $\mu m)$ eyedrop treatment resulted in significantly lower CCT compared to no treatment (125 \pm 73 μ m) and similar to CCT in no injury eyes (78.7 \pm 7.4 μ m, Fig. 7E). The percentage of mice (n = 7-12 per group) with ≤ 20 % CCT change compared to baseline was only 14.3 % for the no treatment group, 80.0 % for the LE drops group, and 90.9 % for the PBA-MC-LE eyedrop group. In addition, corneal opacity areas of commercial LE drops (10.3 \pm 4.0 %) or PBA-MC-LE (8.2 \pm 4.0 %) eyedrop group were significantly less than no treatment group (45.4 \pm 34.4 %, Fig. 7F). On day 7, the percentage of mice (n = 12 per group) with a clear iris margin, indicative of good

corneal transparency, was only 16.7~% in the no treatment group, 64.0~% in the LE eyedrop group, and 83.3~% in the PBA-MC-LE eyedrop group.

After 7 days of treatment, corneal structures were assessed by H&E staining (n = 4-5 per group), immune cell infiltration (CD45⁺) was evaluated by immunohistochemistry (n = 4 per group), and corneal cytokine levels were quantified by qRT-PCR (n = 6 per group). H&E staining of the normal cornea revealed a relatively uniform epithelial layer consisting of 5-7 cell layers, a stroma with parallel collagen bundles and normal stromal thickness (Fig. 7C), and an intact endothelium. In the no treatment group, only 20 % of mice showed minimal corneal damage, while the remaining exhibited signs of severe inflammation, including reduced corneal epithelial layers (only 2-3 cell layers, indicated by white arrows), partial loss of the corneal endothelium in some regions (marked by black arrows), and inflammatory cell infiltration (denoted by white asterisks) (Fig. 7C). Consistent with CCT measured by AS-OCT, H&E staining revealed significant corneal stromal thickening in untreated mice (Fig. 7G), suggesting edema, which is associated with reduced corneal stiffness and elasticity [90]. In contrast, 100 % of injured eyes (n = 4) treated with either commercial LE drops or the PBA-MC-LE eyedrops maintained nearly intact corneal layers, showing no significant structural damage to the corneal epithelium, stromal tissue, or endothelium, normal corneal thickness, and few infiltration of inflammatory cells (Figs. 7C, G). After 7 days, with no treatment, the number of CD45⁺ immune cells (green) in corneal epithelial and stromal layers significantly increased. In contrast, CD45⁺ cells in corneal epithelial and stromal layers were markedly less with LE eyedrops or PBA-MC-LE eyedrop treatment compared to untreated cornea (Figs. 7D, H). Additionally, the levels of inflammatory cytokines, interleukin (IL)-1β, and IL-6 mRNA in the cornea significantly increased in the no treatment group compared to the contralateral (non-injured) eye. However, treatment with commercial LE eyedrops or PBA-MC-LE eyedrops significantly decreased the expression of IL-1 β and IL-6 (Figs. 7I, J). Overall, our results showed reduced inflammation in our corneal inflammation model through treatment with eyedrops composed of PBA-MC-LE that promoted drug retention through mucoadhesive sites and sustained drug release. Importantly, our PBA-MC-LE eyedrop formulation allowed for a significant reduction in dosage frequency as compared to commercial eye drops, from four times to once a day, while still achieving comparable beneficial anti-inflammatory effects. This underscores the promising potential of our MC formulation for clinical translation in a variety of ocular anterior segment pathologies that require sustained anti-inflammatory therapy. However, future larger animal studies or clinical trials are needed for comprehensive validation.

We evaluated the ocular biocompatibility of the PBA-MC-LE eyedrop formulation alongside its efficacy in a mouse model of electrocautery-induced corneal inflammation. Throughout the 7-day treatment period, no apparent adverse effects were observed (Fig. S8). Fluorescein staining results showed epithelial defects were absent from day 2 onward (Fig. S9A). H&E staining confirmed no pathological damage to the retina, which maintained intact histological layers, including the photoreceptor layer (Ph), outer nuclear layer (ONL), inner nuclear layer (INL), and ganglion cell layer (GCL) (Fig. S9B).

4. Conclusions

We have successfully engineered a polymeric micellar eyedrop solution with a high PBA conjugation efficiency to enhance the efficient delivery of LE to the inflamed eye. The mucoadhesive capability of the engineered PBA-MC eyedrops, as confirmed through turbidity and fluorescence studies, *ex vivo* studies, and *in vivo* corneal retention, indicated its ability to adhere to the mucin layer on the surface of the cornea. This adherence suggested that the eyedrop has an increased retention time over the cornea, which could lead to improved therapeutic efficacy and sustained drug delivery. Additionally, due to its

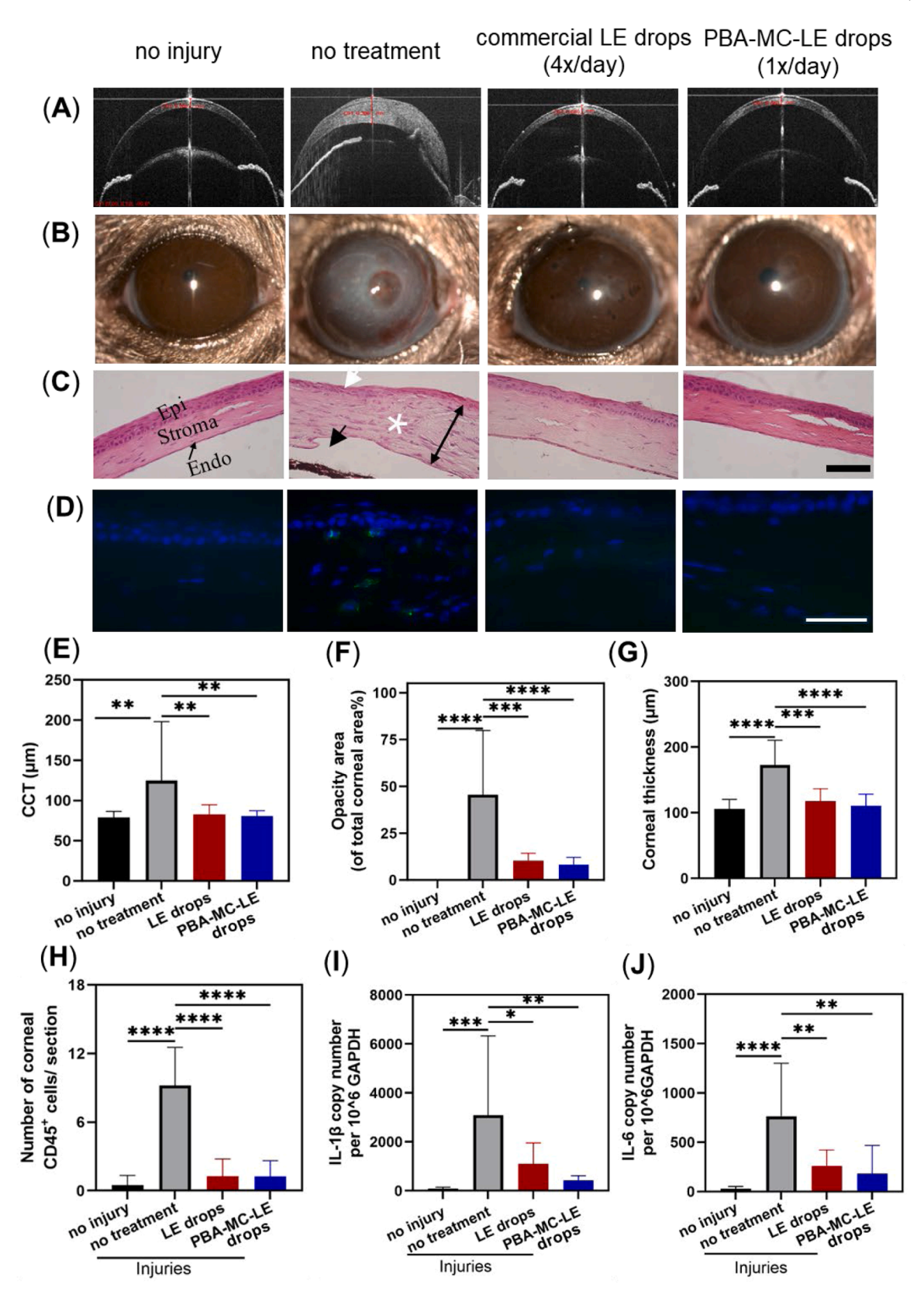


Fig. 7. *In vivo* efficacy studies of PBA-MC-LE eyedrops in a murine model of electrocautery-induced corneal inflammation. (A) Representative AS-OCT images of no injury, no treatment, commercial LE drops (4x/day), and PBA-MC-LE (1x/day) eyedrop groups on day 7; (B) slit lamp photographs on day 7; (C) representative H&E stained images (scale bar: $100 \mu m$) of cornea. Normal corneas (no injury) composed of 3 layers: corneal epithelium (Epi), stromal tissue, and endothelial tissue (Endo) serve as a control; (D) corneal CD45⁺ (green) /DAPI (blue) staining on day 7 (scale bar = $50 \mu m$); (E) quantification of central corneal thickness (CCT) on day 7 by analysis of AS-OCT images; (F) quantification of opacity area on day 7; (G) quantification of corneal thickness (μm) by analysis of H&E stained images; (H) quantification of CD45⁺ positive cells per section. (I) Corneal IL-1 β and (J) IL-6 mRNA levels after 7 days. n = 4–12.

ability to interact with LE through hydrophobic interactions and the hydrolysable lactate chains, it demonstrated a promising potential for sustained drug release for up to 12 days. In addition, *in vitro* and *in vivo* biocompatibility tests ensured its safe utilization for ocular applications. The *in vivo* studies showed that the LE-loaded micellar eyedrop, administered once per day, demonstrated comparable efficacy in treating ocular inflammation to the commercial LE eyedrop (Oceanside®, 0.5% Ophthalmic Suspension), which was administered four times per day. Thus, the engineered micellar eyedrop formulation holds great promise to be used in emergency healthcare and can improve drug bioavailability and patient compliance for efficient treatment of ocular inflammation.

CRediT authorship contribution statement

Yuting Zheng: Writing – review & editing, Writing – original draft, Visualization, Validation, Supervision, Project administration, Methodology, Investigation, Formal analysis, Data curation, Conceptualization. Yimin Gu: Writing - review & editing, Writing - original draft, Validation, Methodology, Investigation, Formal analysis, Data curation. Yavuz Oz: Writing - review & editing, Writing - original draft, Visualization, Validation, Methodology, Investigation, Formal analysis, Data curation. Liangju Kuang: Writing – original draft, Writing – review & editing, Validation, Methodology, Investigation, Formal analysis, Data curation. Ann Yung: Investigation, Formal analysis, Data curation. Seokjoo Lee: Methodology, Formal analysis. Reza Dana: Writing review & editing, Validation, Supervision, Resources, Project administration, Methodology, Investigation, Funding acquisition, Formal analysis, Conceptualization. Nasim Annabi: Writing - review & editing, Writing - original draft, Validation, Supervision, Software, Resources, Project administration, Methodology, Investigation, Funding acquisition, Formal analysis, Conceptualization.

Declaration of competing interest

The author is an Editorial Board Member/Editor-in-Chief/Associate Editor/Guest Editor for *Biomaterials Science, Tissue Engineering: Part B* and was not involved in the editorial review or the decision to publish this article.

The authors declare the following financial interests/personal relationships which may be considered as potential competing interests:

The authors declare the following financial interests/personal relationships which may be considered as potential competing interests: Prof Annabi and Prof Dana hold equity in GelMEDIX Inc.

Acknowledgements

We thank Dr. Francesca Kahale for her assistance with the slit lamp photography and OCT image collection, and Dr. Akitomo Narimatsu for his assistance with tissue harvesting. This work was supported by the Department of Defense (DOD), Vision Research Program (VRP), Investigator Initiated Research Award (W81XWH-21–1–0869), and National Eye Institute/National Institutes of Health Core Grant for Vision Research (P30EY003790).

Supplementary materials

Supplementary material associated with this article can be found, in the online version, at doi:10.1016/j.actbio.2025.05.065.

References

- [1] S.C. Tidke, P. Tidake, A review of corneal blindness: causes and management, Cureus 14 (2022) e30097.
- [2] E.T.E. Cunningham, M. Zierhut, Vision loss in uveitis, Ocul. Immunol. Inflamm. 29 (2021) 1037–1039.

[3] J. Li, J. Yang, Z. Liu, X. Li, Effect of metformin on the level of aqueous humor inflammatory cytokines in patients with cataract, Sci. Rep. 15 (2025) 3672.

- [4] J.T. Rosenbaum, B. Bodaghi, C. Couto, M. Zierhut, N. Acharya, C. Pavesio, M.-L. Tay-Kearney, P. Neri, K. Douglas, S. Pathai, New observations and emerging ideas in diagnosis and management of non-infectious uveitis: a review. Semin. Arthritis Rheum., Elsevier, 2019, pp. 438–445.
- [5] C.R. Harrell, Therapeutic potential of p-MAPPS™ for ocular inflammatory diseases and regeneration of injured corneal and retinal tissue, Int. J. Mol. Sci. 23 (2022) 13528.
- [6] A.C. Bisen, A. Dubey, S. Agrawal, A. Biswas, K.S. Rawat, S. Srivastava, R.S. Bhatta, Recent updates on ocular disease management with ophthalmic ointments, Ther. Deliv. 15 (2024) 463–480.
- [7] D.H. Dang, K.M. Riaz, D. Karamichos, Treatment of non-infectious corneal injury: review of diagnostic agents, therapeutic medications, and future targets, Drugs 82 (2022) 145–167.
- [8] G. Prosperi-Porta, S. Kedzior, B. Muirhead, H. Sheardown, Phenylboronic-acid-based polymeric micelles for mucoadhesive anterior segment ocular drug delivery, Biomacromolecules 17 (2016) 1449–1457.
- [9] O.L. Lanier, M.G. Manfre, C. Bailey, Z. Liu, Z. Sparks, S. Kulkarni, A. Chauhan, Review of approaches for increasing ophthalmic bioavailability for eye drop formulations, Aaps Pharmscitech 22 (2021) 1–16.
- [10] I.A. Khalil, B. Saleh, D.M. Ibrahim, C. Jumelle, A. Yung, R. Dana, N. Annabi, Ciprofloxacin-loaded bioadhesive hydrogels for ocular applications, Biomater. Sci. 8 (2020) 5196–5209.
- [11] G. Fang, X. Yang, Q. Wang, A. Zhang, B. Tang, Hydrogels-based ophthalmic drug delivery systems for treatment of ocular diseases, Mater. Sci. Eng. C. 127 (2021) 112212
- [12] X. Chen, S. Gholizadeh, M. Ghovvati, Z. Wang, M.J. Jellen, A. Mostafavi, R. Dana, N. Annabi, Engineering a drug eluting ocular patch for delivery and sustained release of anti-inflammatory therapeutics, AIChE J 69 (2023) e18067.
- [13] E.B. Souto, S. Doktorovova, E. Gonzalez-Mira, M.A. Egea, M.L. Garcia, Feasibility of lipid nanoparticles for ocular delivery of anti-inflammatory drugs, Curr. Eye Res. 35 (2010) 537–552.
- [14] K.M. Cosert, S. Kim, I. Jalilian, M. Chang, B.L. Gates, K.E. Pinkerton, L.S. Van Winkle, V.K. Raghunathan, B.C. Leonard, S.M. Thomasy, Metallic engineered nanomaterials and ocular toxicity: a current perspective, Pharmaceutics 14 (2022) 981
- [15] D. Berillo, Z. Zharkinbekov, Y. Kim, K. Raziyeva, K. Temirkhanova, A. Saparov, Stimuli-responsive polymers for transdermal, transmucosal and ocular drug delivery, Pharmaceutics 13 (2021) 2050.
- [16] S. Liu, C.N. Chang, M.S. Verma, D. Hileeto, A. Muntz, U. Stahl, J. Woods, L. W. Jones, F.X. Gu, Phenylboronic acid modified mucoadhesive nanoparticle drug carriers facilitate weekly treatment of experimentallyinduced dry eye syndrome, Nano Res 8 (2015) 621–635.
- [17] A. Mandal, R. Bisht, I.D. Rupenthal, A.K. Mitra, Polymeric micelles for ocular drug delivery: from structural frameworks to recent preclinical studies, J. Control. Release, 248 (2017) 96–116.
- [18] Y. Wu, L.K. Vora, D. Mishra, M.F. Adrianto, S. Gade, A.J. Paredes, R.F. Donnelly, T. R.R. Singh, Nanosuspension-loaded dissolving bilayer microneedles for hydrophobic drug delivery to the posterior segment of the eye, Biomater. Adv. 137 (2022) 212267.
- [19] Y. Lee, S. Park, S. Il Kim, K. Lee, W. Ryu, Rapidly detachable microneedles using porous water-soluble layer for ocular drug delivery, Adv. Mater. Technol. 5 (2020) 1901145.
- [20] H. Shi, J. Zhou, Y. Wang, Y. Zhu, D. Lin, L. Lei, S. Vakal, J. Wang, X. Li, A rapid corneal healing microneedle for efficient ocular drug delivery, Small 18 (2022) 2104657.
- [21] P. Gadziński, A. Froelich, M. Wojtyłko, A. Białek, J. Krysztofiak, T. Osmałek, Microneedle-based ocular drug delivery systems–recent advances and challenges, Beilstein J. Nanotechnol. 13 (2022) 1167–1184.
- [22] G. Behl, J. Iqbal, N.J. O'Reilly, P. McLoughlin, L. Fitzhenry, Synthesis and characterization of poly (2-hydroxyethylmethacrylate) contact lenses containing chitosan nanoparticles as an ocular delivery system for dexamethasone sodium phosphate, Pharm. Res. 33 (2016) 1638–1648.
- [23] F.H. Nasr, S. Khoee, M.M. Dehghan, S.S. Chaleshtori, A. Shafiee, Preparation and evaluation of contact lenses embedded with polycaprolactone-based nanoparticles for ocular drug delivery, Biomacromolecules 17 (2016) 485–495.
- [24] Y.M.G. Mohamdeen, A.G. Tabriz, M. Tighsazzadeh, U. Nandi, R. Khalaj, I. Andreadis, J.S. Boateng, D. Douroumis, Development of 3D printed drug-eluting contact lenses, J. Pharm. Pharmacol. 74 (2022) 1467–1476.
- [25] C. Alvarez-Lorenzo, S. Anguiano-Igea, A. Varela-García, M. Vivero-Lopez, A. Concheiro, Bioinspired hydrogels for drug-eluting contact lenses, Acta Biomater 84 (2019) 49–62.
- [26] K. Glover, D. Mishra, S. Gade, L.K. Vora, Y. Wu, A.J. Paredes, R.F. Donnelly, T.R. R. Singh, Microneedles for advanced ocular drug delivery, Adv. Drug Deliv. Rev. 201 (2023) 115082.
- [27] C. Alvarez-Lorenzo, H. Hiratani, A. Concheiro, Contact lenses for drug delivery, Am. J. Drug Deliv. 4 (2006) 131–151.
- [28] S.R. Croy, G.S. Kwon, Polymeric micelles for drug delivery, Curr. Pharm. Des. 12 (2006) 4669–4684.
- [29] S. Gholizadeh, Z. Wang, X. Chen, R. Dana, N. Annabi, Advanced nanodelivery platforms for topical ophthalmic drug delivery, Drug Discov. Today. 26 (2021) 1437–1449.
- [30] R. Suri, S. Beg, K. Kohli, Target strategies for drug delivery bypassing ocular barriers, J. Drug Deliv. Sci. Technol. 55 (2020) 101389.

[31] C. Li, Z. Liu, X. Yan, W. Lu, Y. Liu, Mucin-controlled drug release from mucoadhesive phenylboronic acid-rich nanoparticles, Int. J. Pharm. 479 (2015) 261–264.

- [32] G. Tan, J. Li, Y. Song, Y. Yu, D. Liu, W. Pan, Phenylboronic acid-tethered chondroitin sulfate-based mucoadhesive nanostructured lipid carriers for the treatment of dry eye syndrome, Acta Biomater 99 (2019) 350–362.
- [33] X. Sun, Y. Sheng, K. Li, S. Sai, J. Feng, Y. Li, J. Zhang, J. Han, B. Tian, Mucoadhesive phenylboronic acid conjugated chitosan oligosaccharide-vitamin E copolymer for topical ocular delivery of voriconazole: synthesis, in vitro/vivo evaluation, and mechanism, Acta Biomater 138 (2022) 193–207.
- [34] R. Bernardini, A. Oliva, A. Paganelli, E. Menta, M. Grugni, S. De Munari, L. Goldoni, Stability of boronic esters to hydrolysis: a comparative study, Chem. Lett. 38 (2009) 750–751.
- [35] J.D. Bartlett, B. Horwitz, R. Laibovitz, J.F. Howes, Intraocular pressure response to loteprednol etabonate in known steroid responders, J. Ocul. Pharmacol. Ther. 9 (1993) 157–165.
- [36] E.J. Holland, J.D. Bartlett, M.R. Paterno, D.W. Usner, T.L. Comstock, Effects of loteprednol/tobramycin versus dexamethasone/tobramycin on intraocular pressure in healthy volunteers, Cornea 27 (2008) 50–55.
- [37] G.D. Novack, J. Howes, R.S. Crockett, M.B. Sherwood, Change in intraocular pressure during long-term use of loteprednol etabonate, J. Glaucoma. 7 (1998) 266-269
- [38] C.E. Pavesio, H.H. DeCory, Treatment of ocular inflammatory conditions with loteprednol etabonate, Br. J. Ophthalmol. 92 (2008) 455–459.
- [39] J.D. Sheppard, T.L. Comstock, M.E. Cavet, Impact of the topical ophthalmic corticosteroid loteprednol etabonate on intraocular pressure, Adv. Ther. 33 (2016) 532–552.
- [40] T.L. Comstock, H.H. DeCory, Advances in corticosteroid therapy for ocular inflammation: loteprednol etabonate, Int. J. Inflam. 2012 (2012).
- [41] R. Ferrari, M. Callari, D. Moscatelli, Multiple strategies to produce lipophilic nanoparticles leaving water-soluble poly (HPMA), RSC Adv 5 (2015) 67475–67484.
- [42] M. Talelli, M. Iman, A.K. Varkouhi, C.J.F. Rijcken, R.M. Schiffelers, T. Etrych, K. Ulbrich, C.F. van Nostrum, T. Lammers, G. Storm, Core-crosslinked polymeric micelles with controlled release of covalently entrapped doxorubicin, Biomaterials 31 (2010) 7797–7804.
- [43] L. Marinelli, I. Cacciatore, E. Fornasari, C. Gasbarri, G. Angelini, A. Marrazzo, A. Pandolfi, D. Mandatori, Y. Shi, C.F. Van Nostrum, Preparation and characterization of polymeric micelles loaded with a potential anticancer prodrug, J. Drug Deliv. Sci. Technol. 35 (2016) 24–29.
- [44] O. Naksuriya, Y. Shi, C.F. Van Nostrum, S. Anuchapreeda, W.E. Hennink, S. Okonogi, HPMA-based polymeric micelles for curcumin solubilization and inhibition of cancer cell growth, Eur. J. Pharm. Biopharm. 94 (2015) 501–512.
- [45] L. Chong, Y.-W. Jiang, D. Wang, P. Chang, K. Xu, J. Li, Targeting and repolarizing M2-like tumor-associated macrophage-mediated MR imaging and tumor immunotherapy by biomimetic nanoparticles, J. Nanobiotechnology. 21 (2023) 401.
- [46] B. Srividya, R.M. Cardoza, P.D. Amin, Sustained ophthalmic delivery of ofloxacin from a pH triggered *in situ* gelling system, J. Control. Release. 73 (2001) 205–211.
 [47] G. Horvát, B. Gyarmati, S. Berkó, P. Szabó-Révész, B.Á. Szilágyi, A. Szilágyi,
- [47] G. Horvát, B. Gyarmati, S. Berkó, P. Szabó-Révész, B.Á. Szilágyi, A. Szilágyi, J. Soós, G. Sandri, M.C. Bonferoni, S. Rossi, Thiolated poly (aspartic acid) as potential in situ gelling, ocular mucoadhesive drug delivery system, Eur. J. Pharm. Sci. 67 (2015) 1–11
- [48] R.S. Dave, T.C. Goostrey, M. Ziolkowska, S. Czerny-Holownia, T. Hoare, H. Sheardown, Ocular drug delivery to the anterior segment using nanocarriers: a mucoadhesive/mucopenetrative perspective, J. Control. Release. 336 (2021) 71.88
- [49] M.R. Dana, R. Dai, S. Zhu, J. Yamada, J.W. Streilein, Interleukin-1 receptor antagonist suppresses Langerhans cell activity and promotes ocular immune privilege, Invest. Ophthalmol. Vis. Sci. 39 (1998) 70–77.
- [50] R. Gref, M. Lück, P. Quellec, M. Marchand, E. Dellacherie, S. Harnisch, T. Blunk, R. H. Müller, Stealth'corona-core nanoparticles surface modified by polyethylene glycol (PEG): influences of the corona (PEG chain length and surface density) and of the core composition on phagocytic uptake and plasma protein adsorption, Colloids Surfaces B Biointerfaces 18 (2000) 301–313.
- [51] C. Zhang, J. Li, M. Xiao, D. Wang, Y. Qu, L. Zou, C. Zheng, J. Zhang, Oral colon-targeted mucoadhesive micelles with enzyme-responsive controlled release of curcumin for ulcerative colitis therapy, Chinese Chem. Lett. 33 (2022) 4924–4929.
- [52] D.B. Kaldybekov, P. Tonglairoum, P. Opanasopit, V.V. Khutoryanskiy, Mucoadhesive maleimide-functionalised liposomes for drug delivery to urinary bladder, Eur. J. Pharm. Sci. 111 (2018) 83–90.
- [53] B. Wu, S. Sai, K. Li, X. Sun, J. Han, B. Tian, Maleimide-functionalized phospholipid/Pluronic F127 mixed micelles for efficient ophthalmic delivery of voriconazole against Candida albicans, Colloids Surfaces B Biointerfaces 209 (2022) 112180.
- [54] D.B. Kaldybekov, S.K. Filippov, A. Radulescu, V.V. Khutoryanskiy, Maleimidefunctionalised PLGA-PEG nanoparticles as mucoadhesive carriers for intravesical drug delivery, Eur. J. Pharm. Biopharm. 143 (2019) 24–34.
- [55] K. Albrecht, A. Bernkop-Schnürch, Thiomers: forms, functions and applications to nanomedicine, Nanomedicine 2 (2007) 41–50.
- [56] A. Mahmood, M. Lanthaler, F. Laffleur, C.W. Huck, A. Bernkop-Schnürch, Thiolated chitosan micelles: highly mucoadhesive drug carriers, Carbohydr. Polym. 167 (2017) 250–258.
- [57] A. Sanchez, E. Pedroso, A. Grandas, Maleimide-dimethylfuran exo adducts: effective maleimide protection in the synthesis of oligonucleotide conjugates, Org. Lett. 13 (2011) 4364–4367.

[58] N. Hock, G.F. Racaniello, S. Aspinall, N. Denora, V.V. Khutoryanskiy, A. Bernkop-Schnürch, Thiolated nanoparticles for biomedical applications: mimicking the workhorses of our body, Adv. Sci. 9 (2022) 2102451.

- [59] Y. Zheng, Y. Oz, Y. Gu, N. Ahamad, K. Shariati, J. Chevalier, D. Kapur, N. Annabi, Rational design of polymeric micelles for targeted therapeutic delivery, Nano Today 55 (2024) 102147.
- [60] D.R. Janagam, L. Wu, T.L. Lowe, Nanoparticles for drug delivery to the anterior segment of the eye, Adv. Drug Deliv. Rev. 122 (2017) 31–64.
- [61] M.J.E. Fischer, Amine coupling through EDC/NHS: a practical approach, Surf. Plasmon Reson. Methods Protoc. (2010) 55–73.
- [62] M. D'Este, D. Eglin, M. Alini, A systematic analysis of DMTMM vs EDC/NHS for ligation of amines to hyaluronan in water, Carbohydr. Polym. 108 (2014) 239–246.
- [63] C. Wang, Q. Yan, H.-B. Liu, X.-H. Zhou, S.-J. Xiao, Different EDC/NHS activation mechanisms between PAA and PMAA brushes and the following amidation reactions, Langmuir 27 (2011) 12058–12068.
- [64] M. Bagheri, J. Bresseleers, A. Varela-Moreira, O. Sandre, S.A. Meeuwissen, R. M. Schiffelers, J.M. Metselaar, C.F. Van Nostrum, J.C.M. van Hest, W.E. Hennink, effect of formulation and processing parameters on the size of mPEG-b-p (HPMA-Bz) polymeric micelles, Langmuir 34 (2018) 15495–15506.
- [65] Y.-C. Chen, C.-L. Lo, Y.-F. Lin, G.-H. Hsiue, Rapamycin encapsulated in dual-responsive micelles for cancer therapy, Biomaterials 34 (2013) 1115–1127.
- [66] Y.-C. Chen, L.-C. Liao, P.-L. Lu, C.-L. Lo, H.-C. Tsai, C.-Y. Huang, K.-C. Wei, T.-C. Yen, G.-H. Hsiue, The accumulation of dual pH and temperature responsive micelles in tumors, Biomaterials 33 (2012) 4576–4588.
- [67] O. Soga, C.F. van Nostrum, M. Fens, C.J.F. Rijcken, R.M. Schiffelers, G. Storm, W. E. Hennink, Thermosensitive and biodegradable polymeric micelles for paclitaxel delivery, J. Control. Release. 103 (2005) 341–353.
- [68] H. Huang, X. Zhang, J. Yu, J. Zeng, P.R. Chang, H. Xu, J. Huang, Fabrication and reduction-sensitive behavior of polyion complex nano-micelles based on PEGconjugated polymer containing disulfide bonds as a potential carrier of anti-tumor paclitaxel, Colloids Surfaces B Biointerfaces 110 (2013) 59–65.
- [69] J. Logie, S.C. Owen, C.K. McLaughlin, M.S. Shoichet, PEG-graft density controls polymeric nanoparticle micelle stability, Chem. Mater. 26 (2014) 2847–2855.
- [70] M.E. Durgun, S. Güngör, Y. Özsoy, Micelles: promising ocular drug carriers for anterior and posterior segment diseases, J. Ocul. Pharmacol. Ther. 36 (2020) 323–341.
- [71] J. Jiao, Polyoxyethylated nonionic surfactants and their applications in topical ocular drug delivery, Adv. Drug Deliv. Rev. 60 (2008) 1663–1673.
- [72] P.A. Simmons, J.G. Vehige, Investigating the potential benefits of a new artificial tear formulation combining two polymers, Clin. Ophthalmol. 11 (2017) 1637–1642.
- [73] C. Gagliano, V. Papa, R. Amato, G. Malaguarnera, T. Avitabile, Measurement of the retention time of different ophthalmic formulations with ultrahigh-resolution optical coherence tomography, Curr. Eye Res. 43 (2018) 499–502.
- [74] K. Han, O.E. Woghiren, R. Priefer, Surface tension examination of various liquid oral, nasal, and ophthalmic dosage forms, Chem. Cent. J. 10 (2016) 1–5.
- [75] M.C. Carnahan, D.A. Goldstein, Ocular complications of topical, peri-ocular, and systemic corticosteroids, Curr. Opin. Ophthalmol. 11 (2000) 478–483.
- [76] A. Popov, Mucus-penetrating particles and the role of ocular mucus as a barrier to micro-and nanosuspensions, J. Ocul. Pharmacol. Ther. 36 (2020) 366–375.
- [77] M. Shin, K. Kim, W. Shim, J.W. Yang, H. Lee, Tannic acid as a degradable mucoadhesive compound, ACS Biomater. Sci. Eng. 2 (2016) 687–696.
- [78] R.P. Brannigan, V.V. Khutoryanskiy, Progress and current trends in the synthesis of novel polymers with enhanced mucoadhesive properties, Macromol. Biosci. 19 (2019) 1900194
- [79] A. Guzman-Aranguez, P. Argüeso, Structure and biological roles of mucin-type Oglycans at the ocular surface, Ocul. Surf. 8 (2010) 8–17.
- glycans at the ocular surface, Ocul. Surf. 8 (2010) 8–17.

 [80] S. Liu, M.D. Dozois, C.N. Chang, A. Ahmad, D.L.T. Ng, D. Hileeto, H. Liang, M.-M. Reyad, S. Boyd, L.W. Jones, Prolonged ocular retention of mucoadhesive nanoparticle eye drop formulation enables treatment of eye diseases using significantly reduced dosage, Mol. Pharm. 13 (2016) 2897–2905.
- [81] J. Zhou, R. Wang, W. Su, L. Zhang, A. Li, T. Jiao, Efficient detection of glucose by graphene-based non-enzymatic sensing material based on carbon dot, Colloids Surfaces A Physicochem. Eng. Asp. 647 (2022) 129122.
- [82] D.-E. Wang, J. Yan, J. Jiang, X. Liu, C. Tian, J. Xu, M.-S. Yuan, X. Han, J. Wang, Polydiacetylene liposomes with phenylboronic acid tags: a fluorescence turn-on sensor for sialic acid detection and cell-surface glycan imaging, Nanoscale 10 (2018) 4570–4578.
- [83] M. Sonnaert, I. Papantoniou, F.P. Luyten, J. Schrooten, Quantitative validation of the presto blue™ metabolic assay for online monitoring of cell proliferation in a 3D perfusion bioreactor system, Tissue Eng. Part C Methods. 21 (2015) 519–529.
- [84] K. Lu, D. Wang, G. Zou, Y. Wu, F. Li, Q. Song, Y. Sun, A multifunctional composite hydrogel that sequentially modulates the process of bone healing and guides the repair of bone defects, Biomed. Mater. 19 (2024) 35010.
- [85] D. Lee, Q. Lu, S.D. Sommerfeld, A. Chan, N.G. Menon, T.A. Schmidt, J.H. Elisseeff, A. Singh, Targeted delivery of hyaluronic acid to the ocular surface by a polymerpeptide conjugate system for dry eye disease, Acta Biomater 55 (2017) 163–171.
- [86] A. Račić, D. Krajišnik, Biopolymers in mucoadhesive eye drops for treatment of dry eye and allergic conditions: application and perspectives, Pharmaceutics 15 (2023) 470.
- [87] C. Guarise, L. Acquasaliente, G. Pasut, M. Pavan, M. Soato, G. Garofolin, R. Beninatto, E. Giacomel, E. Sartori, D. Galesso, The role of high molecular weight hyaluronic acid in mucoadhesion on an ocular surface model, J. Mech. Behav. Biomed. Mater. 143 (2023) 105908.
- [88] S. Glogowski, E. Lowe, R. Siou-Mermet, T. Ong, M. Richardson, Prolonged exposure to loteprednol etabonate in human tear fluid and rabbit ocular tissues

- following topical ocular administration of Lotemax gel, 0.5 %, J. Ocul. Pharmacol. Ther. 30 (2014) 66–73.
- [89] X. Zhao, I. Seah, K. Xue, W. Wong, Q.S.W. Tan, X. Ma, Q. Lin, J.Y.C. Lim, Z. Liu, B. H. Parikh, Antiangiogenic nanomicelles for the topical delivery of aflibercept to treat retinal neovascular disease, Adv. Mater. 34 (2022) 2108360.
- [90] S. Li, S. Zhang, F. Fang, J. Bai, H. Sun, L. Chen, Y. Fu, A stemness-enhanced eye drop stimulates corneal regeneration via sustained release of Versican and providing lubricated substrate, Adv. Funct. Mater. 35 (2025) 2411735.
- [91] S.C. Saccà, A.M. Roszkowska, A. Izzotti, Environmental light and endogenous antioxidants as the main determinants of non-cancer ocular diseases, Mutat. Res. Mutat. Res. 752 (2013) 153–171.